Current Research (2023) Newfoundland and Labrador Department of Industry, Energy and Technology
Geological Survey, Report 23-1, pages 99-125

WHITE MICA ZONATION PATTERNS ASSOCIATED WITH HYBRID BIMODAL-FELSIC VMS SYSTEMS: EXAMPLES FROM THE TULKS VOLCANIC AND BUCHANS–ROBERTS ARM BELTS, CENTRAL NEWFOUNDLAND

G.W. Sparkes and J.G. Hinchey
Mineral Deposits Section

ABSTRACT

Both, the Tulks Volcanic Belt (TVB) and the Buchans–Roberts Arm Belt (BRAB), are host to volcanogenic massive sulphide (VMS) occurrences, some of which, locally, display a spatial association with the development of aluminous alteration of the immediate footwall rocks to the massive sulphide mineralization. Earlier, these occurrences were classified as hybrid bimodal-felsic VMS systems, given their association with aluminous alteration. The type examples of this style of mineralization within the region include the Daniels Pond and Bobbys Pond deposits (and related Bobbys Pond sulphur prospect; TVB) and the Mary March prospect (BRAB). Short wavelength infrared (SWIR) investigations of drillcore from these areas outline the zonation of argillic alteration (paragonite/muscovite ± kaolinite ± halloysite ± dickite ± montmorillonite) proximal to mineralized zones, in addition to locally identifying well-developed, advanced argillic alteration (pyrophyllite ± dickite ± kaolinite ± alunite) within hotter, more acidic portions of the overall hydrothermal systems. For both the TVB and BRAB, these zones of advanced argillic alteration are generally devoid of significant base- or precious-metal enrichment. Instead, VMS mineralization develops marginal to such zones, where it is associated with argillic alteration assemblages (paragonite–paragonitic-illite–montmorillonite).

*The SWIR data highlight several common alteration assemblages (*e.g.*, paragonitic-illite–montmorillonite) developed in footwall rocks proximal to massive sulphide mineralization. In addition, characteristic shifts in the Al-OH wavelength feature, to shorter wavelengths with decreasing distance from mineralization, highlight the increasingly acidic hydrothermal conditions associated with the development of the mineralized horizon. The characterization of these alteration features around known occurrences of hybrid bimodal-felsic VMS mineralization provides valuable insight into the conditions associated with the overall mineralizing environment. These features may aid in the evaluation of other regional alteration targets with respect to highlighting potential mineralizing environments elsewhere.*

INTRODUCTION

The Tulks Volcanic Belt (TVB) and the southwestern portion of the Buchans–Roberts Arm Belt (BRAB) host examples of hybrid bimodal-felsic styles of volcanogenic massive sulphide (VMS) mineralization (Hinchey, 2011; Sparkes, 2022). Within the TVB, these systems are locally associated with the development of aluminous alteration proximal to VMS mineralization (*e.g.*, Daniels Pond and Bobbys Pond deposits). In the BRAB, this type of VMS system has only recently been recognized, but is also associated with aluminous alteration, spatially associated with the development of VMS mineralization (*e.g.*, Mary March prospect). The overall model for hybrid bimodal-felsic VMS systems is characterized by the development of argillic and advanced argillic alteration, within the footwall rocks, to massive sulphide mineralization (Galley *et al.*, 2007; Figure 1). White mica alteration within the footwall of these systems is commonly referred to as "sericite". However, the use of short wavelength infrared (SWIR) spectrometry enables the subdivision of this sericitic alteration into distinct mineral assemblages (*e.g.*, paragonite, muscovite and phengite), as well as providing a means of accurately identifying minerals associated with advanced argillic alteration (*e.g.*, pyrophyllite, alunite, kaolinite, dickite).

Although the development of advanced argillic alteration assemblages in association with VMS mineralization is rare, the presence of these minerals provides insight regarding the hydrothermal conditions related to their formation, as these minerals are only stable under acidic conditions (Gifkins *et al.*, 2005; Hedenquist and Arribas, 2022).

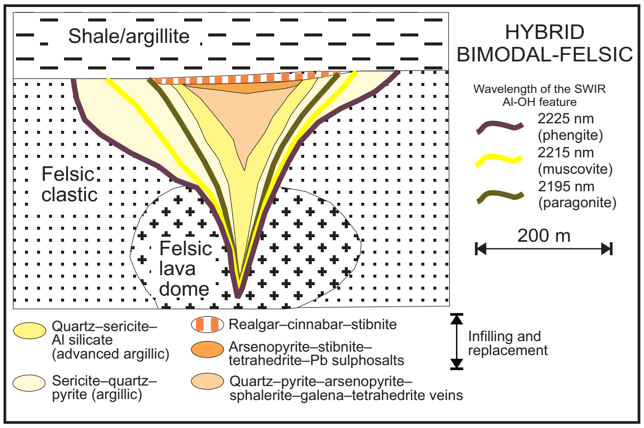

Figure 1. *Model outlining the development of argillic to advanced argillic alteration within the footwall zone of a hybrid bimodal-felsic VMS system (modified from Galley* et al.*, 2007) and the generalized white mica zonation patterns as defined by the position of the SWIR Al-OH wavelength feature as observed in this study.*

The development of these acidic conditions may indicate the influence of magmatic-derived hydrothermal fluids within the VMS environment (*e.g.*, Sillitoe *et al.*, 1996; Hannington *et al.*, 1999; Huston and Kamprad, 2001). This would account for the local enrichment of precious metals (Au, Ag) and the typical epithermal suite of elements observed in such systems (*e.g.*, As, Bi, Hg, Sb, Se, Sn and Te, Brueckner *et al.*, 2014, 2016; Gill *et al.*, 2016; Pilote *et al.*, 2016). The following discussion provides insight through the SWIR investigation of areas that were previously interpreted as being dominated by aluminous alteration (*e.g.*, Daniels Pond and Bobbys Pond), and others that were largely interpreted to be dominated by "sericite" alteration but were found to contain advanced argillic assemblages (*e.g.*, Mary March prospect).

This report is largely based on short wavelength infrared (SWIR) spectral data obtained from drillcore. The collection of systematic, downhole, SWIR data allows for the accurate determination of variations within the alteration mineralogy, which, in turn, provides a better understanding of the spatial relationships between the alteration and the development of massive sulphide mineralization. In addition, SWIR spectrometry provides the ability to obtain mineralogical information on the crystallinity and/or compositional variations associated with certain mineral groups, such as white micas (*e.g.*, paragonite, muscovite and phengite). Illite variants of these white mica minerals are expressed by the spectral software (The Spectral Geologist; TSG™) as either paragonitic-illite, muscovitic-illite, or phengitic-illite (*see* below). The variation in the Al-OH absorption feature (~2200 nm) is one example of a calculated scalar from the spectral data that can be utilized to gain insight regarding the compositional differences within various white mica minerals (*e.g.*, paragonite (2180–2195 nm), muscovite (2195–2215 nm) and phengite (2215–2225 nm); Pontual *et al.*, 1997; AusSpec, 2008). Sodic mica (paragonite) is characterized by shorter wavelengths, whereas muscovite and phengite are representative of more potassic and Fe-Mg micas at longer wavelengths, respectively (Herrmann *et al.*, 2001; Yang *et al.*, 2011). The position of the Al-OH feature also can be used as a hydrothermal pH indicator, with shorter wavelengths representative of more acidic hydrothermal conditions (Halley *et al.*, 2015).

Spectral measurements were collected using either a TerraSpec® Pro or TerraSpec® Halo spectrometer, and these spectra were subsequently processed using The Spectral Geologist (TSG™) software (version 8.0.7.4) to obtain mineral identifications. This software provides the two most abundant minerals present (Min 1 and Min 2) for individual spectral analysis by comparing each spectra to a reference library of known minerals. Within this report, the principal focus deals with the white mica zonation patterns proximal to VMS mineralization that were historically described as being dominated by either "sericite" or aluminous alteration. For the basis of this discussion, advanced argillic alteration is characterized by the mineral assemblage pyrophyllite ± dickite ± kaolinite ± alunite, whereas argillic alteration is characterized by paragonite/muscovite ± kaolinite ± halloysite ± dickite ± montmorillonite ± chlorite (modified after Gifkins *et al.* (2005) and references therein).

NORTHERN TULKS VOLCANIC BELT

REGIONAL GEOLOGY

The northern TVB (Figure 2) contains a wide variety of rock types, dominated by felsic, intermediate, and mafic volcanic rocks including ash tuff, lapillistone, agglomerates, massive to flow-banded rhyolite, and rhyolite breccias with local, commonly amygdaloidal, dykes and sills. Sedimentary rocks are also present and include black shale, graphitic argillite, greywacke, and iron formation. The region also contains intrusive bodies generally interpreted to be synvolcanic. The northern TVB has undergone moderate to strong deformation, and sub-greenschist to greenschist-facies metamorphism throughout. Primary textures are usually obliterated by well-developed, bedding-parallel, foliations. Stratigraphy typically strikes to the southwest–northeast and dips steeply to the northwest, with a prominent regional foliation defined by the alignment of chlorite and white micas. The belt is transected by late shear zones and faults that have variable orientations.

The VMS mineralization in the northern TVB is characteristically associated with felsic volcanic rocks including

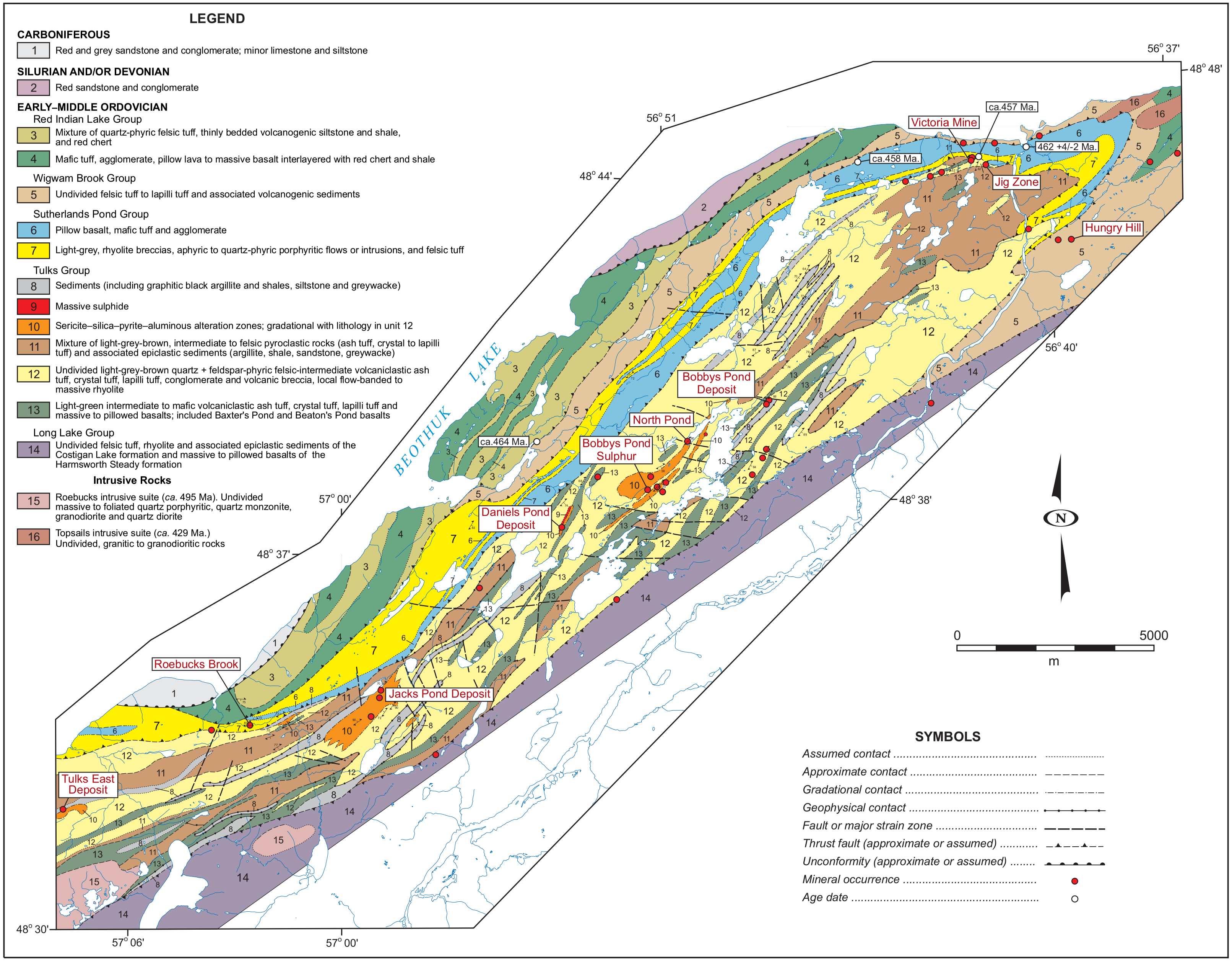

Figure 2. *Regional geology map of the northern Tulks Volcanic Belt, outlining the location of the Daniels Pond and Bobbys Pond VMS deposits and the Bobbys Pond sulphur prospect, along with zones of sericite–silica–pyrite–aluminous alteration (from Hinchey, 2011).*

ash- and quartz ± feldspar crystal-tuff, rhyolite, rhyolitic breccias, volcano-sedimentary debris-flow deposits, and lesser mafic volcanic rocks, hosted within epiclastic sedimentary basin(s). The local abundance of bimodal sills, commonly amygdaloidal, which are broadly synchronous with the volcano-sedimentary sequence, suggests a possible arc-rift or back-arc basin tectonic setting for parts of the belt. This region is host to several VMS deposits, as well as numerous other prospects and zones of alteration; the most notable deposits are the Daniels Pond and Bobbys Pond deposits (Figure 2). Mineralization at these deposits is associated with intense white mica–silica–pyrite alteration and less well-developed chloritic and minor illite and halloysite alteration (Hinchey, 2011). The mineralization is considered to have formed in both the exhalative and sub-seafloor replacement environments.

LOCAL GEOLOGY AND VMS MINERALIZATION

Daniels Pond Deposit

The Daniels Pond deposit is hosted by a sequence of intermediate to mafic ash- and crystal- to lapilli tuff. Alteration is dominated by white mica–silica–pyrite, and minor aluminous (paragonite, halloysite) alteration, and local chlorite–carbonate alteration. Historically, zones of intense alteration in drillcore, which in the vicinity of the deposit makes identification of the original rock type difficult, have been logged as pyrophyllite (*e.g.*, Barbour *et al.*, 1990). Unlike many of the other deposits in the TVB, the immediate stratigraphic footwall is dominated by mafic to intermediate volcanic and volcaniclastic rocks, although the surrounding rock types, in both the hanging wall and along strike, are dominated by felsic volcanic rocks. The host rocks are steeply dipping, and based on the observed grading in epiclastic rocks, the sequence is overturned to the northwest. The stratigraphic footwall rocks, sitting structurally above the ore horizon, consist of intensely altered intermediate to mafic ash- to lapilli-tuff, and intermediate to mafic amygdaloidal sills. The stratigraphic hanging wall (structural footwall), consists of debris flows containing quartz-phyric felsic volcanic, fine-grained argillite, and massive sulphide clasts. The presence of sulphide clasts within the debris flow may suggest an exhalative origin for much of the mineralization. The remainder of the stratigraphic hanging-wall sequence consists of variably altered intermediate to felsic ash, lapilli tuff and associated epiclastic sedimentary rocks. The proportion of sedimentary rocks (dominantly graphitic argillite and greywacke), as observed in drillcore, increases substantially toward the northeast, near a pyrite-rich part of the deposit (*see* below). The mafic to intermediate volcanic and epiclastic host rocks are intensely altered to white mica–silica–carbonate–chlorite– pyrite, and little, if any, of the original minerals are preserved.

Massive sulphide mineralization at Daniels Pond is contained within two lenses, a pyrite-dominant, weakly base-metal-rich lens to the northeast and a base-metal-rich lens to the southwest. The massive sulphide lenses are confined to a narrow belt of highly strained rocks trending north–south, and are traceable along strike for up to 1.1 km (Figure 3). The base-metal-rich sulphides consist of sphalerite–galena–pyrite ± chalcopyrite. These sulphides have been structurally modified and show tectonic banding and recrystallization. Mineralization at Daniels Pond contains elevated silver in comparison with other VMS mineralization within the TVB, which occurs in both the native form and as tennantite–tetrahedrite (Mckenzie *et al.*, 1993). The presence of coarse-grained pyrite, which overprints banded sulphides, indicates extensive recrystallization. Gangue mineralogy is variable with a mixture of quartz–carbonate ± barite distributed throughout the lenses (*see* also McKenzie *et al.*, 1993; Noranda, 1998). The ore in the northern lens is dominated by fine-grained pyrite having fine-scale tectonic (?) banding; this pyrite is noted to contain elevated gold ranging from 500–1500 ppb (McKenzie *et al.*, 1993). Quartz–carbonate veinlets commonly infill crosscutting fractures and locally contain minor remobilized copper mineralization in the form of chalcopyrite.

The aluminous alteration displays a spatial association with the development of massive sulphide mineralization, but is itself generally only weakly mineralized with respect to base metals and commonly displays low-grade enrichment of gold. Locally, the aluminous alteration has been identified to host up to 1.2% Zn, 0.17% Cu, 3.2% As, 655 g/t Ag, 74 ppm Mo and >200 ppm Sb (Plate 1), but this is rare for samples containing in excess of 20% Al_2O_3 (*see* Hinchey, 2011). The aluminous alteration is locally host to higher grade zinc enrichment, where the alteration is transitional into zones of chlorite-dominated alteration, which is the main host to the highest grade massive sulphide mineralization (Plate 2).

Alteration is predominantly confined to an area of intensely sheared volcanic rocks in the immediate footwall to the deposit, with minor white mica–carbonate alteration locally present in the hanging-wall rocks. The alteration at the Daniels Pond deposit appears different than that observed at other deposits in the TVB, in part due to the local presence of aluminous alteration with localized values of up to 36.5% Al_2O_3 (Hinchey, 2011). Footwall alteration is best developed within intensely sheared intermediate to mafic volcanic tuffs, and consists of variable amounts of white mica, silica, chlorite, carbonate and aluminous alteration, and is associated with pyrite and base-metal stringer sulphides. Locally, black chlorite, aluminous alteration, ± white mica occurs in the immediate footwall of the deposit, implying a vent proximal acidic mineralizing environment

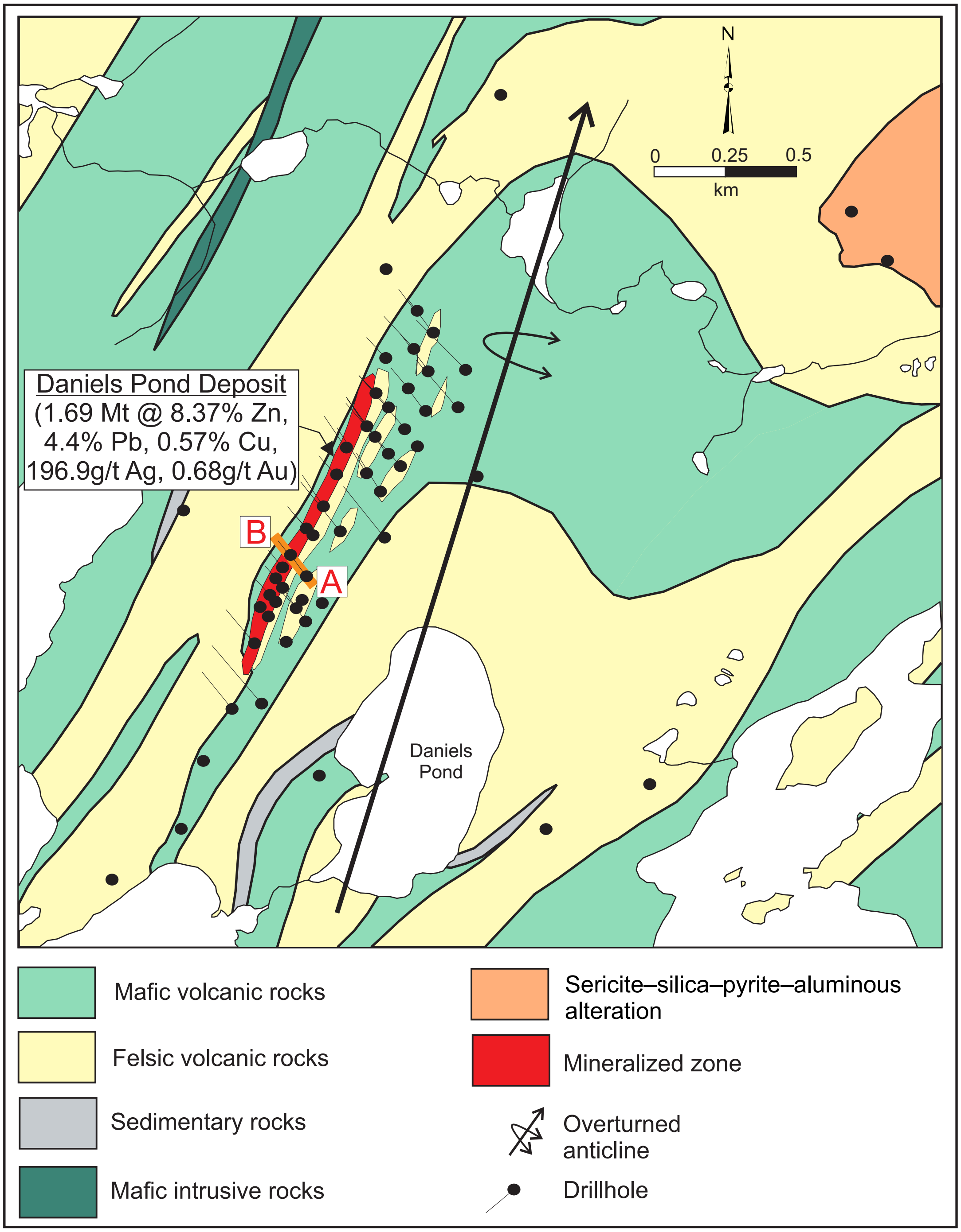

Figure 3. *Geology of the Daniels Pond deposit (modified from McKenzie* et al. *(1993) and Dadson* et al. *(2004)).*

(Hinchey, 2011), and the proportion and intensity of the alteration is greater in the area of the base-metal lens than in the area of the pyrite lens, to the northeast. More regional-scale, less intense alteration is recognized in both the hanging wall and footwall stratigraphy distal to the main mineralized horizon. This alteration is considered to be of regional hydrothermal origin and consists of fine-grained white mica and carbonate alteration.

Bobbys Pond Deposit

The Bobbys Pond deposit occurs in a stratigraphic sequence similar to that at the Daniels Pond deposit, but the two cannot be unequivocally correlated. This deposit is hosted in variably altered, bimodal volcanic sequences, dominated by aphyric to quartz-porphyritic rhyolite, rhyolite breccia, felsic ash-, crystal- and lapilli-tuff, and intercalated

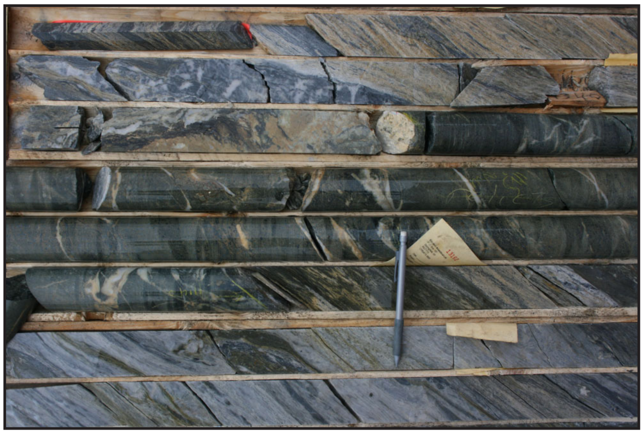

Plate 1. *Aluminous alteration locally returning values of up to 25.15% Al_2O_3, 1.2% Zn, 0.17% Cu, 3.2% As, 655 g/t Ag, >200 ppm Sb, 155 Cd and 74 ppm Mo over 0.2 m (upper left hand corner; JHC-07-083; Hinchey, 2011). A company assay covering this interval returned 2.1 g/t Au and 294.5 g/t Ag over 2.1 m (Sawitzky and Dadson, 2003). Note the aluminous alteration below the relic, relatively unaltered mafic volcanic host rocks (centre of photo) is anomalous throughout with respect to Zn, Ag and Au. Daniels Pond deposit; DDH DN-02-10 @ ~134 m.*

epiclastic sediments (graphitic argillite and greywacke) and minimal mafic volcanic rocks (Figure 4). The preponderance of rhyolite in the sequence distinguishes it from the volcaniclastic-dominated deposits farther south (*e.g.*, Daniels Pond, Tulks East, *etc.*), and may suggest a more vent proximal environment of formation. Additionally, mafic volcanic rocks are not present in the immediate stratigraphic succession hosting the Bobbys Pond deposit, differentiating it from other deposits in the belt. Strong white mica–carbonate–pyrite–silica alteration and local aluminous alteration are observed in proximity to the sulphide lenses.

The stratigraphic footwall sequence is dominated by aphyric to quartz-phyric rhyolite and associated felsic ash- to crystal-tuff, lapilli-tuff, and related epiclastic sediments. "Jig-saw-fit" rhyolitic breccias are common in the footwall sequence and are interpreted to result from natural inflation processes associated with emplacement of felsic flows or domes. Similar textures are associated with felsic domes at the Duck Pond deposit (*e.g.*, Squires *et al.*, 2001). It was suggested by Stewart and Beischer (1993) that some of the porphyritic rhyolites may actually be intrusions.

The hanging-wall sequence is dominated by variably altered rhyolite breccias with intercalated felsic ash- and

Plate 2. *White mica-dominated alteration enveloping a zone of more chlorite-dominated alteration. Also shown are the point locations of spectral measurements with associated mineralogy and the approximate location of company assay results for zinc over this interval (assay data from Barbour* et al.*, 1990). DDH DN-06, 51 to 79 m depth.*

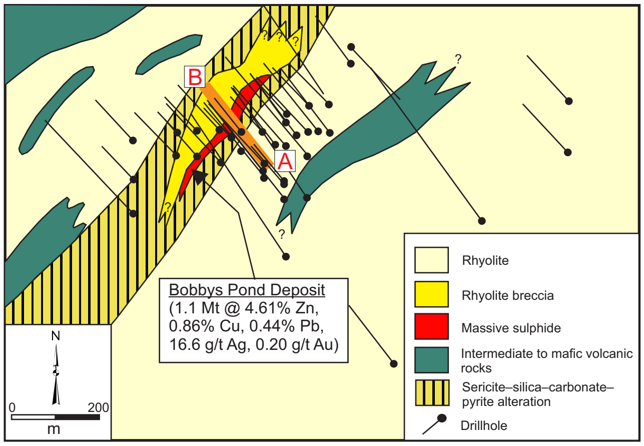

Figure 4. *Geology of the Bobbys Pond deposit (modified from Stewart and Beisher (1993) and Agnerian (2007)).*

crystal tuff to lapilli tuff, and lesser amounts of siliceous sedimentary rocks. The rocks in both the stratigraphic hanging wall and footwall of the deposit are strongly deformed, and are locally altered to sericite schists.

Massive sulphide mineralization occurs in at least four sulphide lenses, ranging from less than 1 to approximately 10 m, within an approximately 100-m-wide zone of moderate to intense alteration. Intense shearing, coupled with the local presence of fault gouge in the immediate vicinity of the mineralization, imply that the ore horizon "stratigraphy" may actually represent a series of transposed slices, resulting in repetition of massive sulphide layers and associated alteration. However, some variations in sulphide compositions were observed between the lenses, and there are also subtle contrasts in their host rock types. Such variations can be explained by lateral variations in sulphide lenses, such as demonstrated at Daniels Pond. Sulphides are dominated by pyrite and lesser honey-coloured sphalerite, chalcopyrite and galena (Plate 3). Locally, sulphides pervasively replace the rhyolite suggesting a replacement style of mineralization, whereas elsewhere the presence of fine-grained, mineralized siliceous sedimentary rocks may suggest an exhalative style of mineralization.

The alteration observed at the Bobbys Pond deposit, as with the Daniels Pond deposit, mostly represents local hydrothermal alteration associated with the development of VMS mineralization. Most of the alteration, and associated sulphide mineralization, occur within a zone of strong deformation developed within strongly altered sericitic schists. As with the Daniels Pond deposit, hydrothermal alteration is localized and there is no well-defined footwall alteration system associated with a typical feeder zone. The intensity of alteration and its affect on the competency of the footwall rocks likely acted to focus deformation in this region. Footwall alteration proximal to massive sulphides is dominated by silica–white mica–carbonate–pyrite alteration and local chlorite alteration. Historically, drill logs for the area have noted possible pyrophyllite alteration hosted within the footwall felsic volcanic rocks (*e.g.*, Regular, 2006). Carbonate alteration increases significantly in proximity to the massive sulphides as replacement of primary feldspar, and is more intense than that at other deposits elsewhere in the TVB. Hanging-wall alteration at Bobbys Pond is weakly defined by variable amounts of albite, chlorite, and carbonate alteration along with ubiquitous silicification.

Bobbys Pond Sulphur Prospect

The Bobbys Pond sulphur prospect is located 2.5 km northeast of the Daniels Pond deposit and 5.6 km southwest of the Bobbys Pond deposit (Figure 2). This occurrence consists of felsic volcanic rocks hosting the local development of advanced argillic alteration (*e.g.*, pyrophyllite, alunite, kaolinite and dickite), native sulphur, topaz, orpiment and possible stibnite. The occurrence also exhibits textures suggestive of an epithermal environment, in addition to typical VMS-style mineralization. When viewed in conjunction with the Daniels Pond and Bobbys Pond deposits, which also contain locally acidic, aluminous alteration (*see* above), this hybrid epithermal-VMS style of alteration and mineralization extends over a strike length of 8 km.

The Bobbys Pond sulphur prospect contains abundant argillic to advanced argillic alteration with intense silicification, alunite, native sulphur, and topaz occurring on surface, with orpiment and possible stibnite occurring at depth. The prospect typically lacks VMS-style alteration or mineralization, although massive pyrite mineralization is locally observed in drillcore (Plate 4). As such, the sulphur prospect has historically been viewed as a unique epithermal-style

Plate 3. *Massive sulphide mineralization locally assaying up to 36% Zn over 1 m; DDH 77537 at ~175 m depth (from Hinchey, 2011).*

Plate 4. *Laminated massive pyrite developed within the zone of pyrophyllite-dominated advanced argillic alteration. Note the massive pyrite is associated with anomalous gold (70 ppb over 1 m); DDH BP-05 @ ~107 m depth, Bobbys Pond sulphur prospect.*

mineralizing event in the TVB, superimposed on the older VMS mineralization. As alunite is not uncommon within weakly metamorphosed VMS mineralized terrains (*e.g.*, Morne Bossa deposit; stockwork deposits of the green tuff belt in Japan; *see* Hannington *et al.*, 1999 and references therein), the observed field relationships suggest that alunite may have been (meta?) stable within some of the northern TVB prospects, perhaps preserved due to the associated intense silicification. Vuggy quartz textures also point to an "epithermal-style" of mineralization, potentially indicative of boiling and shallow depths.

SWIR INVESTIGATIONS OF FOOTWALL ATLTERATION ZONES

Daniels Pond Deposit

Downhole spectral data collected from drillhole DN-02-02, Daniels Pond deposit, highlights the overall abundance of muscovite–Fe-Mg chlorite alteration within the tuffaceous rocks marginal to the main zone of hydrothermal alteration (Figure 5). The development of paragonitic illite within the footwall alteration zone marks the onset of the aluminous alteration, with local values of up to 36.5% Al_2O_3 (Hinchey, 2011). This zone is also associated with an overall decrease of the Al-OH wavelength from ~2206 nm at 70 m depth, to approximately 2198 nm at 130 m, indicating increasingly acidic hydrothermal conditions proximal to mineralization (Figure 5). Below ~135 m, within the paragonitic illite-dominated argillic alteration zone, the Al-OH values remain fairly consistent indicating similar hydrothermal conditions (*i.e.*, temperature and acidity) throughout the main zone of footwall alteration associated with mineralization. Within the footwall alteration, proximal to the massive sulphide mineralization, spectral data highlights the presence of montmorillonite (Figure 5).

The main zone of high-grade mineralization is characterized by Fe-Mg chlorite alteration similar to the relationships described above (*e.g.*, Plate 2). Below the mineralized horizon (structural footwall; stratigraphic hanging wall), Al-OH values are observed to gradually shift to longer wavelengths with increasing depth (*i.e.*, moving up section) before transitioning back to background, muscovite-dominated, white mica alteration (~235 m). Carbonate, in the form of siderite, is also characteristic of the hanging-wall environment, along with the notable absence of montmorillonite (Figure 5).

Similar spectral features were observed in drillhole DN-06, which intersected a significant thickness of footwall argillic alteration (paragonitic illite–montmorillonite; Figure 6). Here, similar elevated values of alumina are associated with the development of paragonitic illite–white mica alteration, which is host to anomalous zinc enrichment throughout, indicative of the footwall alteration zone. The relatively sharp but conformable transition into the hanging-wall environment is associated with a notable absence of structurally bound water within the spectral data, indicating less hydrous white mica development above the mineralized horizon (Figure 7).

Bobbys Pond Deposit

A single drillhole, evaluated from the Bobbys Pond area, has several common characteristics with the Daniels Pond alteration data. Spectral data collected from drillhole MOA-05-01, indicate the hole collared into paragonitic illite–montmorillonite-dominated argillic alteration (Figure 8). This alteration continues downhole to ~70 m; however the Al-OH values only display a marked shift from background values (~2196 nm) to shorter wavelengths (~2190 nm) between 55 to 70 m depth. This overall shift displays a similar trend of shorter wavelength Al-OH values developed proximal to mineralization and related alteration as was observed in the area of the Daniels Pond deposit. At 70-m depth, there is a sharp shift in the Al-OH values from ~2190 nm, to longer wavelengths of ~2197 nm. This shift corresponds with noted fault gouge in drillcore and is indicative of a faulted contact juxtaposing contrasting zones of hydrothermal alteration (Figure 8).

The mineralized zone, representing the zone from 70 to 110 m, is dominated by muscovite alteration, however these rocks are characterized overall by a poor spectral response because of increased silicification of the host rock. Lower limits of the mineralized zone are marked by a high-strain zone, which corresponds with a sharp shift in Al-OH values

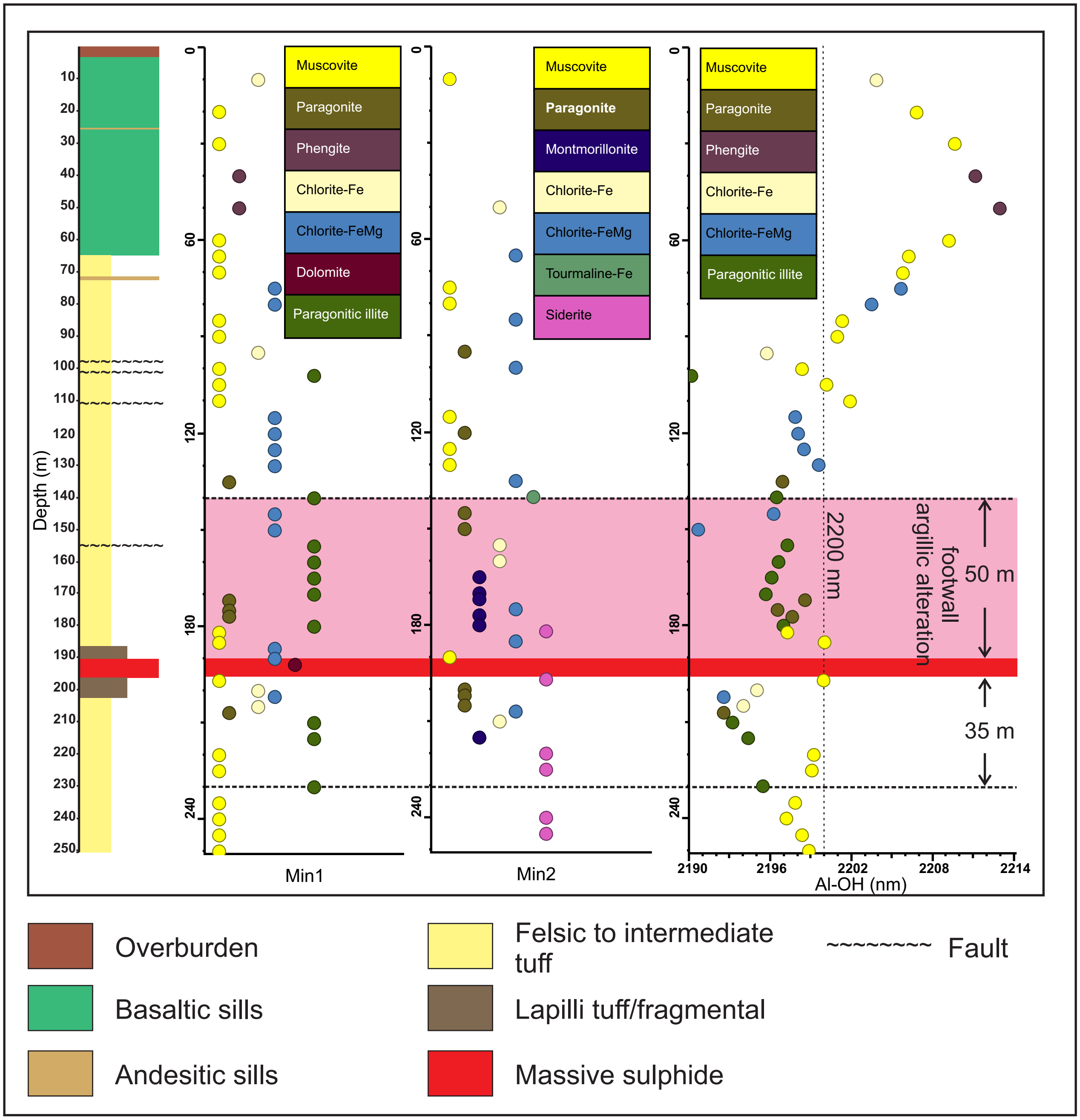

Figure 5. *Strip log for DDH DN-02-02 outlining the distribution of the white mica-dominated alteration in association with VMS mineralization; Daniels Pond deposit. Min 1 and Min 2 represent the two most abundant minerals based on the spectral data as determined from the TSG results. The variation in the calculated Al-OH scalar is shown. Note, the stratigraphy youngs downhole.*

back to shorter wavelengths, similar to those noted above the mineralized zone, indicating the presence of a faulted contact (Figure 8). Below the mineralized horizon, the felsic volcanic rocks, characterized by argillic alteration assemblages, consist of paragonite and paragonitic illite along with carbonate minerals, but lacks montmorillonite, similar to that noted within the immediate hanging wall of the Daniels Pond deposit. Spectral measurements from the footwall zone display prominent structurally bound water features (~1900 nm), which become less prominent within the silicified mineralized zone as well as within the inferred hanging-wall rocks (Figure 9). The similar spectral characteristics of the footwall rocks relative to those of the Daniels Pond deposit support drillhole MOA-05-01 collaring into

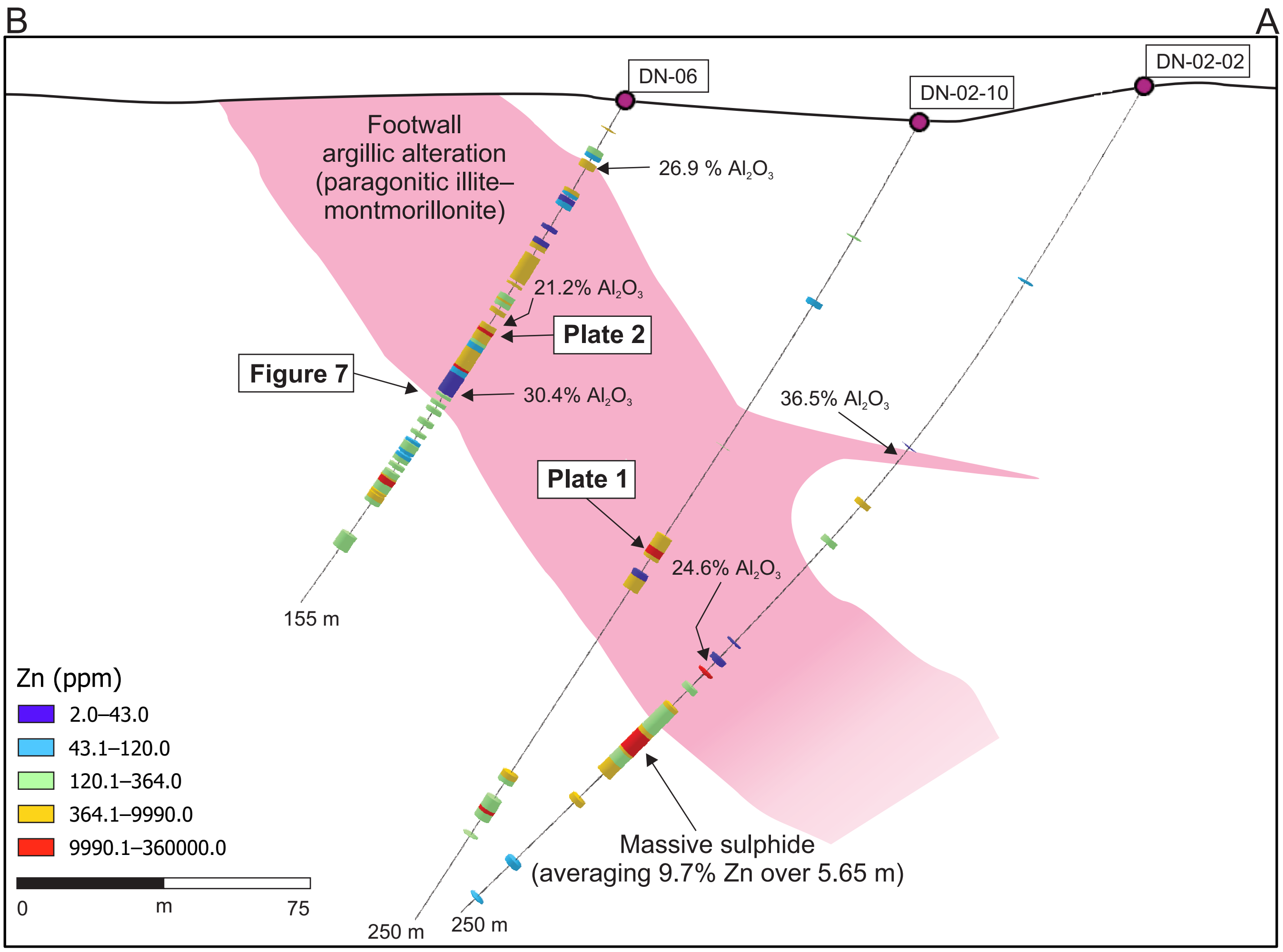

Figure 6. *Schematic cross-section of the Daniels Pond deposit, outlining the distribution of zinc values from industry assay data relative to the defined distribution of the footwall argillic alteration zone based on spectra data from drillholes DN-06 and DN-02-02. Also shown are the Al_2O_3 values for samples containing >20% Al_2O_3 from whole-rock samples of Hinchey (2011). Note the occurrence of massive sulphide mineralization beneath the moderately southeast-dipping zone of paragonitic illite–montmorillonite-dominated argillic alteration. For the reference location of the section* see *Figure 3. Assay data compiled from (Barbour* et al.*, 1990; Sawitzky and Dadson, 2003).*

the footwall and proceeding into the hanging wall toward the bottom of the drillhole (Figure 10).

Bobbys Pond Sulphur Prospect

Two drillholes from the Bobbys Pond sulphur prospect were investigated using the SWIR data, which identified the presence of advanced argillic alteration assemblages (pyrophyllite, alunite, kaolinite and dickite) hosted within felsic volcanic rocks. This zone of advanced argillic alteration is enveloped by extensive paragonite-dominated white mica alteration (Figure 11). The Al-OH values shift toward shorter wavelengths upon approaching zones of pyrophyllite-dominated alteration, from ~2194 to ~2188 nm, highlighting the increasingly acidic hydrothermal conditions associated with the formation of the advanced argillic alteration (Figure 11). A thin layer of locally laminated pyrite, up to 1-m thick (Plate 4) is intercalated with the main zone of pyrophyllite alteration and is presumed to represent exhalative VMS-related mineralization (Figure 11). This massive pyrite is weakly anomalous with respect to gold (70 ppb; Barbour *et al.*, 1991).

The two drillholes examined display intense alteration for their entire length and therefore provided minimal information regarding the overall mineral zonation patterns of the area. However, distal from the main prospect, drillholes along strike of the advanced argillic alteration (*e.g.*, DDH BP-06, located 3.7 km to the northeast) are dominated by phengitic white mica-altered felsic volcanic rocks having

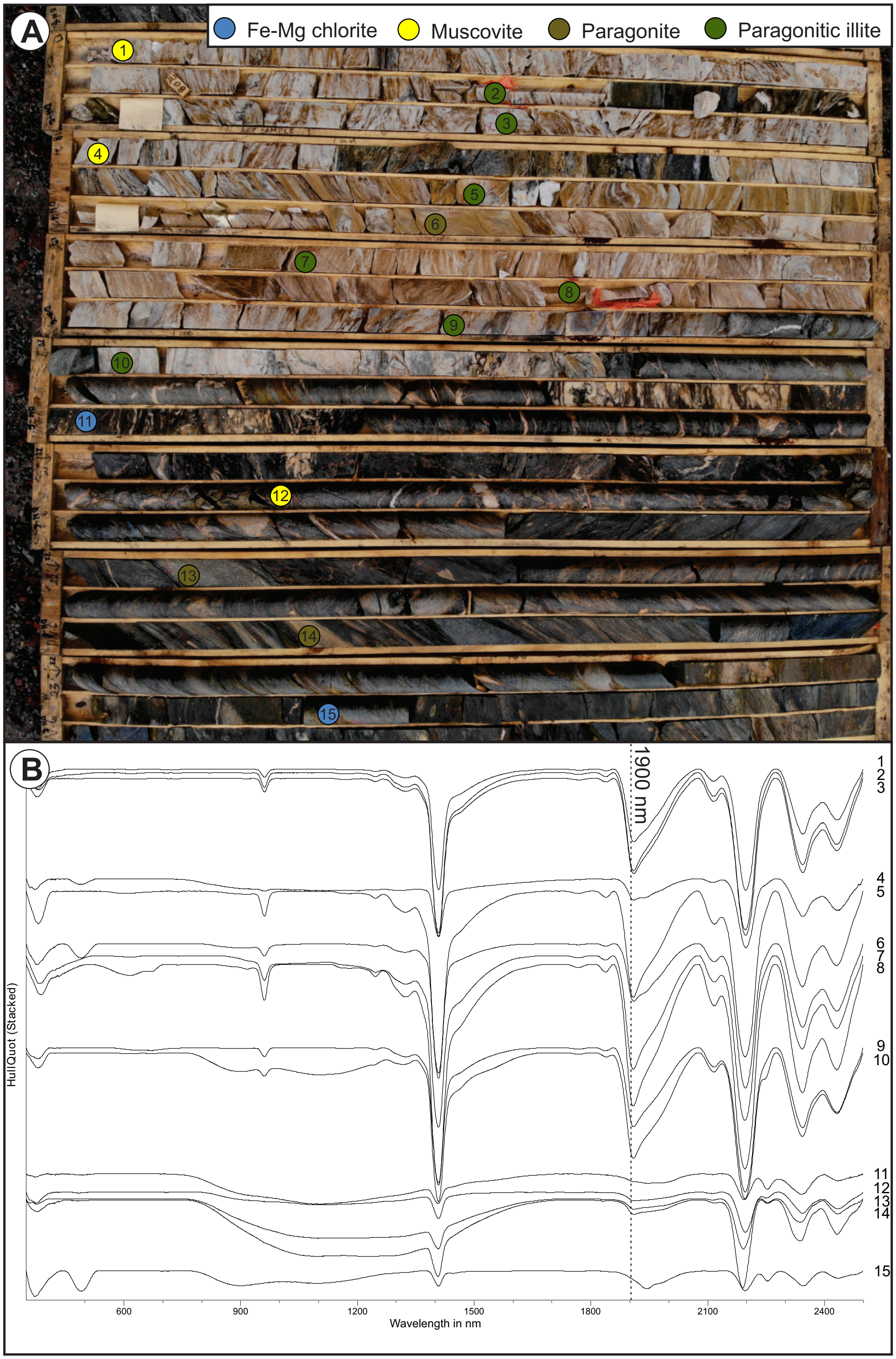

Figure 7. *A) Photo showing the sharp transition into the hanging-wall zone (dark green); DDH DN-06, from 74 to 104 m depth. Also shown are the location of spectral measurements and their corresponding mineralogy; B) Stacked spectral measurements shown in (A), outlining the abrupt termination of the 1900 nm water feature (between spectra 10 and 11) associated with the transition into the hanging-wall environment.*

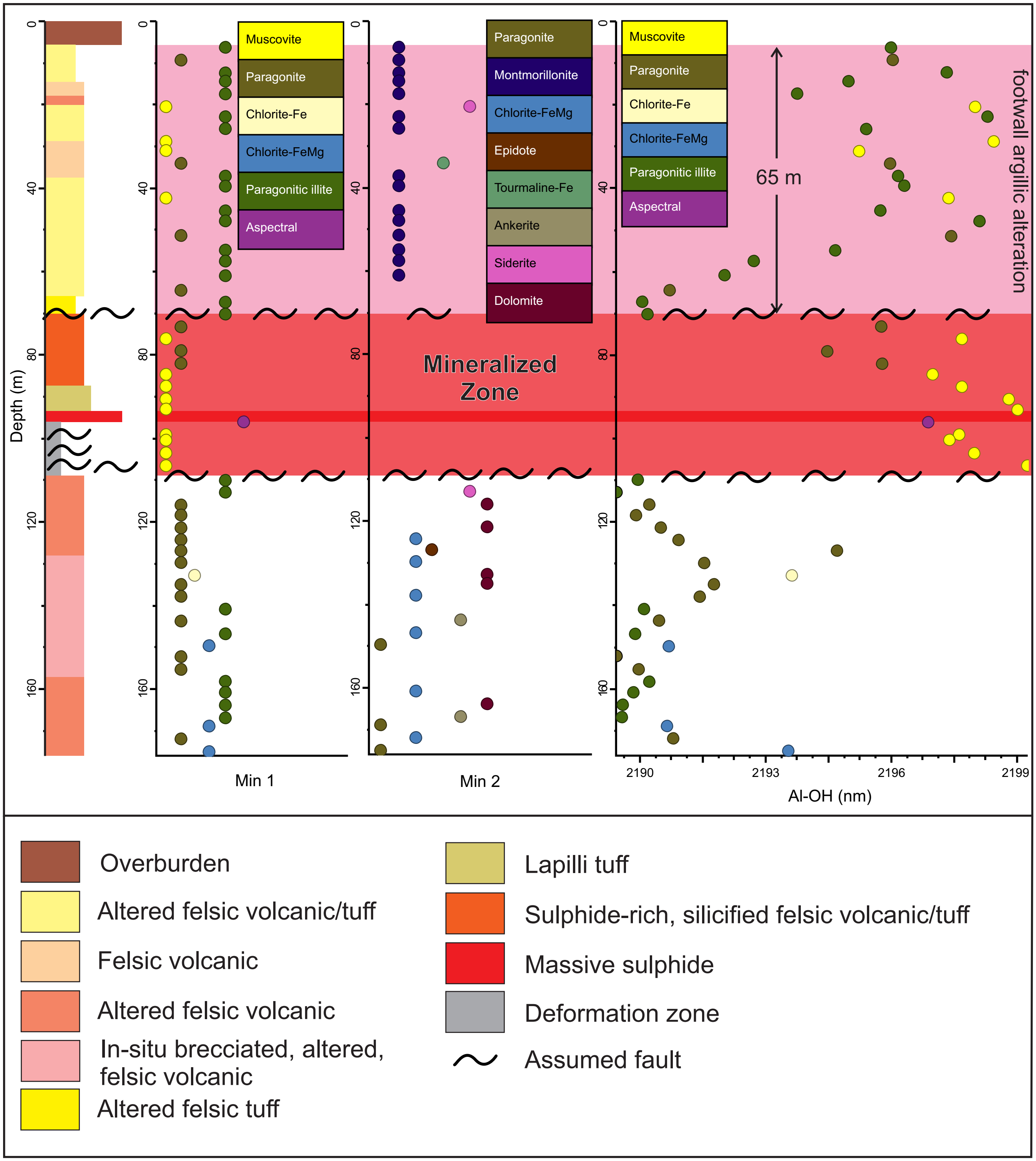

Figure 8. *Strip log for DDH MOA-05-01 outlining the distribution of the white mica-dominated alteration in association with VMS mineralization; Bobbys Pond deposit. Min 1 and Min 2 represent the two most abundant minerals based on the spectral data as determined from the TSG results. The variation in the calculated Al-OH scalar is shown. Note, the stratigraphy youngs downhole.*

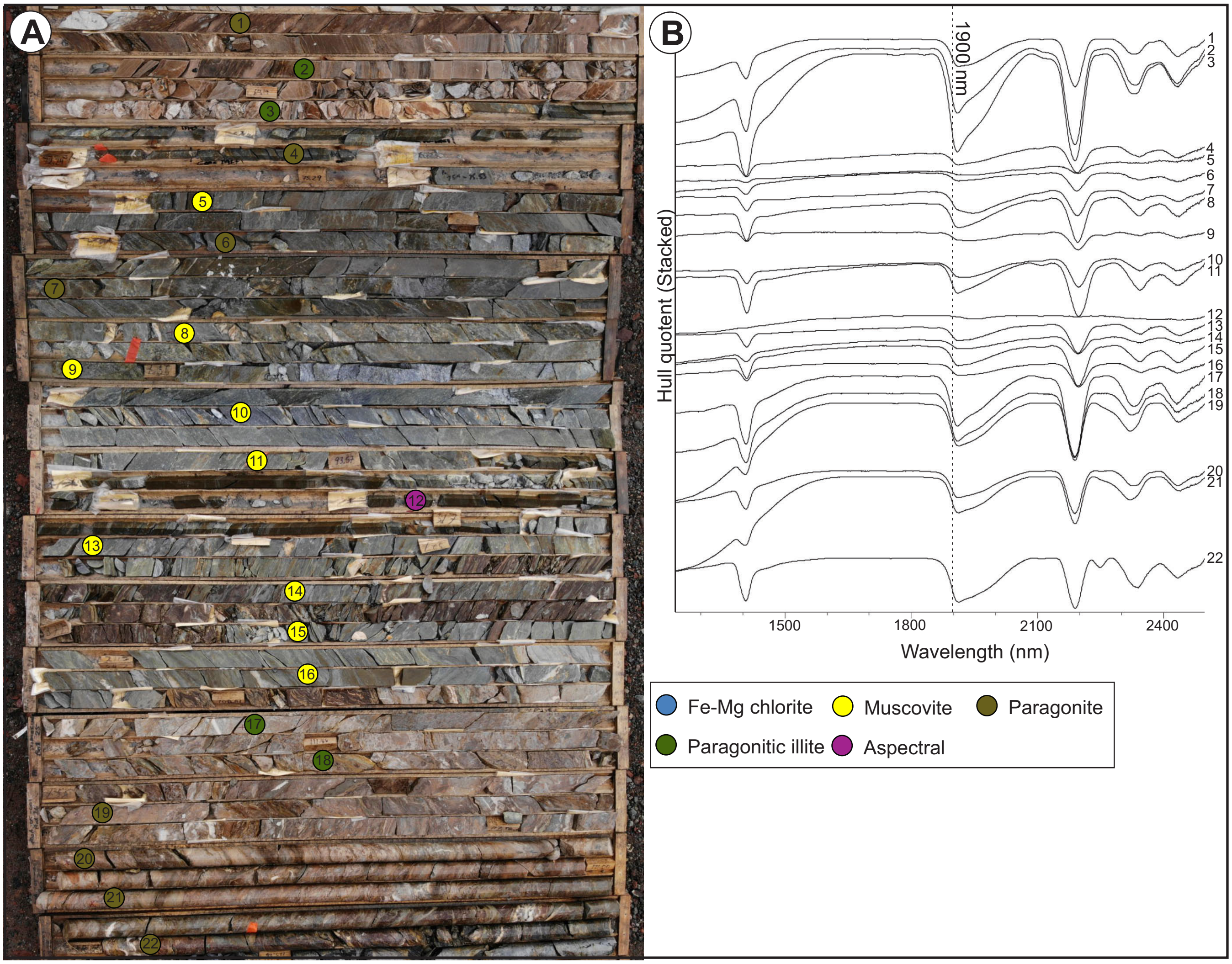

Figure 9. *A) Photograph showing the transition from the footwall zone, through the mineralized zone and into the hanging-wall zone; DDH MOA-05-01, from 64 to 124 m depth. Also shown are the location of spectral measurements and their corresponding mineralogy; B) Stacked spectral measurements shown in (A), outlining the prominent 1900 nm water feature associated with the footwall alteration (spectra 1-3), the reduced spectral signatures associated with the silicified mineralized zone (spectra 4-16), and the paragonite dominated hanging-wall rocks (spectra 17-22).*

Al-OH values of ~2220 nm. These rocks are inferred to be representative of the relatively unaltered regional background signature of the host felsic volcanic sequence.

BUCHANS–ROBERTS ARM BELT

REGIONAL GEOLOGY

The geology of the southern BRAB, primarily confined to the area north of Beothuk Lake, has most recently been discussed by Zagorevski and Rogers (2008, 2009) and Zagorevski *et al.* (2007, 2015, 2016). From this, the geology of the area has been subdivided into five units, consisting of: the Lloyds/Harry's River Ophiolite and Hungry Mountain complexes, and the Buchans, Mary March Brook and the Red Indian Lake groups (Figure 12). Only the Mary March Brook and the Red Indian Lake groups are discussed, as they have relevance to the current study.

The Mary March Brook group consists of bimodal tholeiitic and calc-alkalic volcanic rocks. The formation of tholeiitic rhyolite cryptodomes and coeval island-arc tholeiitic basalts are accompanied by the deposition of rare polymictic debris flows and locally developed hydrothermal alteration and VMS mineralization (Zagorevski and Rogers, 2008, 2009). These rocks conformably overlie bimodal calc-alkalic volcanic rocks. The Mary March Brook group, formed within a back-arc or intra-arc rift setting, has been

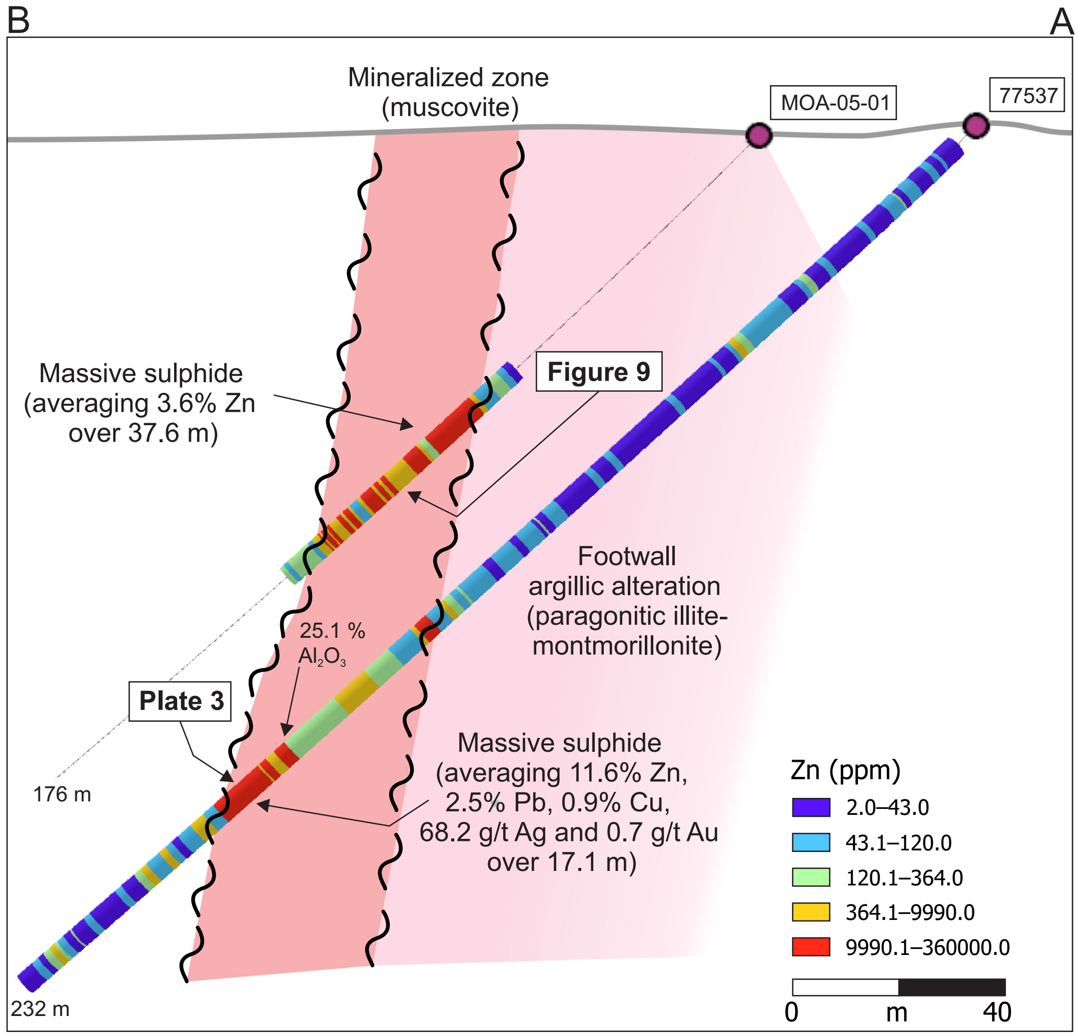

Figure 10. *Schematic cross-section of the Bobbys Pond deposit, outlining the distribution of zinc values from industry assay data relative to the distribution of the footwall argillic alteration zone based on spectra data from DDH MOA-05-01. For the location of section* see *Figure 4. Assay data compiled from Bell* et al. *(1989), Stewart and Beischer (1993) and Regular (2006). Note DDH 77537 is projected 50 m southeast onto the plane of the section; this hole is discussed in detail by Hinchey (2011).*

dated at 461.5 ± 4 Ma (Zagorevski *et al.*, 2015, 2016). This group is host to localized VMS mineralization and sericitic alteration zones, which include Beaver Pond, Seal Pond, Little Sandy, Tower and the Woodman's Brook prospects (Sparkes, 2022 and references therein).

The Red Indian Lake Group is composed of tholeiitic mafic, and overlying calc-alkalic bimodal, volcanic rocks, with the two sequences locally separated by polymictic conglomerate (Zagorevski *et al.*, 2006; Zagorevski and Rogers, 2008, 2009). Rocks at the base of this group are composed of island-arc tholeiities to back-arc basin basalts, along with minor felsic volcanic rocks, formed within a rifted arc or back-arc type setting (Zagorevski *et al.*, 2006). Rocks included within the Red Indian Lake Group have produced ages ranging from 465 ± 4 to 462 +2/-9 Ma (Zagorevski *et al.*, 2015) and host several notable VMS occurrences, which include the Mary March and Connell prospects (Sparkes, 2022 and references therein).

LOCAL GEOLOGY AND VMS MINERALIZATION

Mary March Prospect

The Mary March prospect, hosted within a locally bimodal sequence of mafic, intermediate and felsic volcanic rocks of the Red Indian Lake Group, consists of flows and related volcaniclastic deposits. The volcanic sequence is primarily dominated by locally pillowed mafic volcanic rocks and mafic to intermediate hyaloclastite breccia, and lesser, locally flow-banded, rhyolite and related hyaloclastite. The emplacement of the rhyolite unit displays a spatial associa-

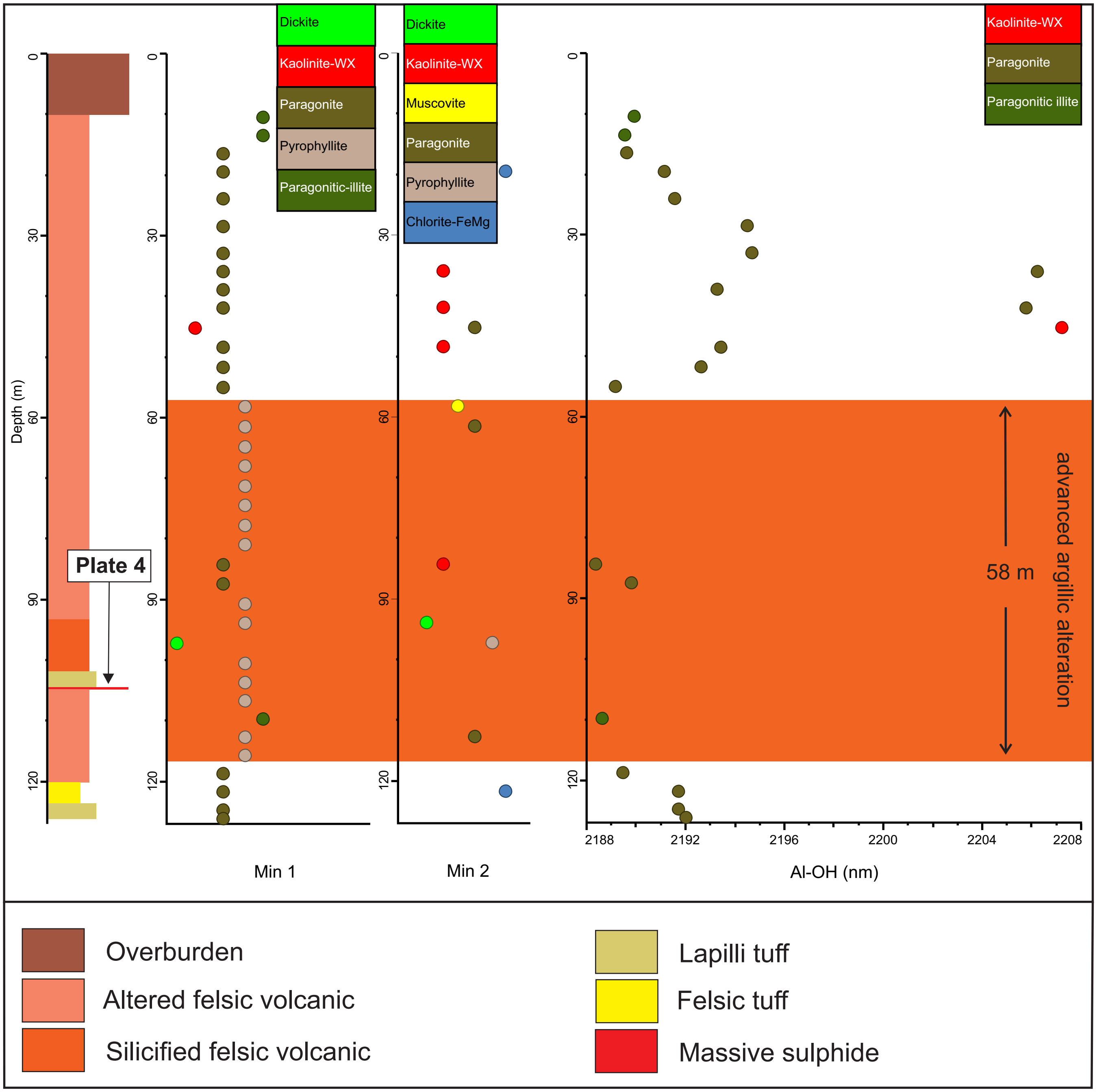

Figure 11. *Representative strip log for DDH BP-05 outlining the distribution of white mica-dominated alteration proximal to well-developed advanced argillic alteration (pyrophyllite-dominated) and locally developed massive sulphide; Bobbys Pond sulphur prospect. Min 1 and Min 2 represent the two most abundant minerals based on the spectral data as determined from the TSG results. The variation in the calculated Al-OH scalar is shown.*

tion with the formation of advanced argillic alteration and localized VMS mineralization, traced along strike, for up to 2 km. This advanced argillic alteration and related massive sulphide mineralization is largely hosted in volcaniclastic units, marginal to the main rhyolite unit, and consist of lapilli tuff, tuff breccia and interbedded volcaniclastic sandstone and siltstone. The aerial distribution of the advanced argillic and marginal argillic alteration surrounding the Mary March area is associated with a pronounced aeromagnetic low, and has a strike length of up to 3 km. This area forms one of the most significant zones of hydrothermal alteration within the region, and given the development of rhyolite flows and

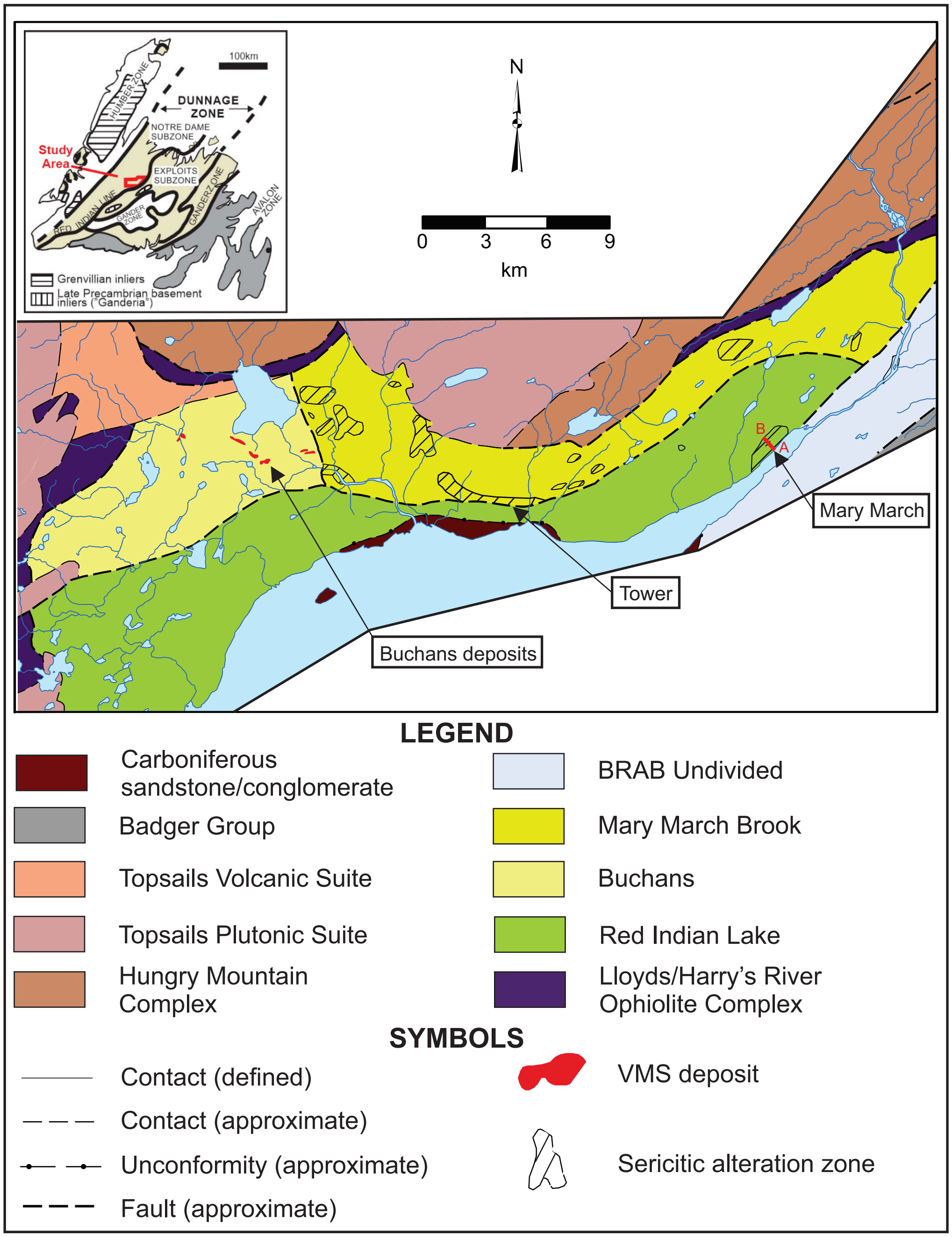

Figure 12. *Regional compilation map outlining the geology and location of select alteration zones relative to the Buchans VMS deposits; geology modified from Zagorevski* et al. *(2015). Note the alteration zones are drawn to encompass drillhole collar locations that are reported to have intersected white mica alteration at depth. The cross-section (A-B) at the Mary March prospect represents the location of Figure 13. BRAB=Buchans–Roberts Arm belt.*

related advanced argillic alteration, is indicative of a vent proximal environment.

The area of the Mary March prospect is divisible into three main structural panels, separated by two significant fault structures, the Mary March (Plate 5A) and the Nancy April (Plate 5B) thrust faults (Figure 13). These northwest steeply dipping thrust faults locally emplace stratigraphic footwall rocks within the structural hanging wall of VMS-related mineralization along the Mary March thrust fault, and result in the structural duplication of the mineralized horizon and related advanced argillic alteration along the Nancy April thrust fault. The rhyolite unit, which locally displays well-developed flow banding and perlitic fracturing

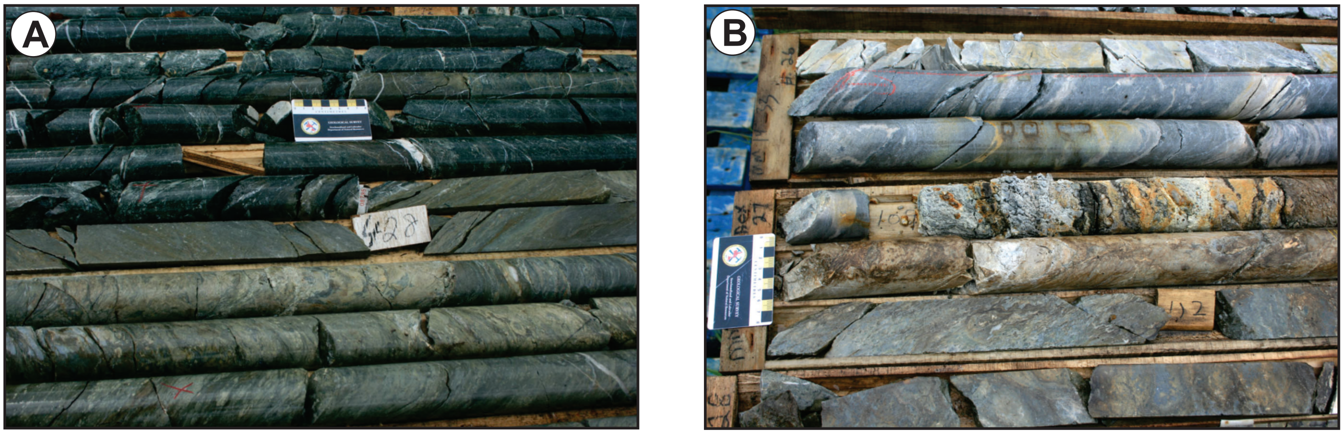

Plate 5. *A) Photo of the Mary March thrust fault separating overlying chlorite-altered mafic volcanic rocks (top; dark green) from the underlying phengite-altered volcaniclastic rocks of the footwall felsic to intermediate volcanic sequence (bottom; light green). DDH MM-19-036, 428 m depth, Mary March prospect; B) Photo of the Nancy April thrust fault separating pyrophyllite-altered intermediate tuff breccia from underlying, phengite-altered mafic volcanic rocks (Figure 13); DDH MM-14-033, 108 m depth, Mary March prospect. Note the development of fault gouge at the location of the thrust fault.*

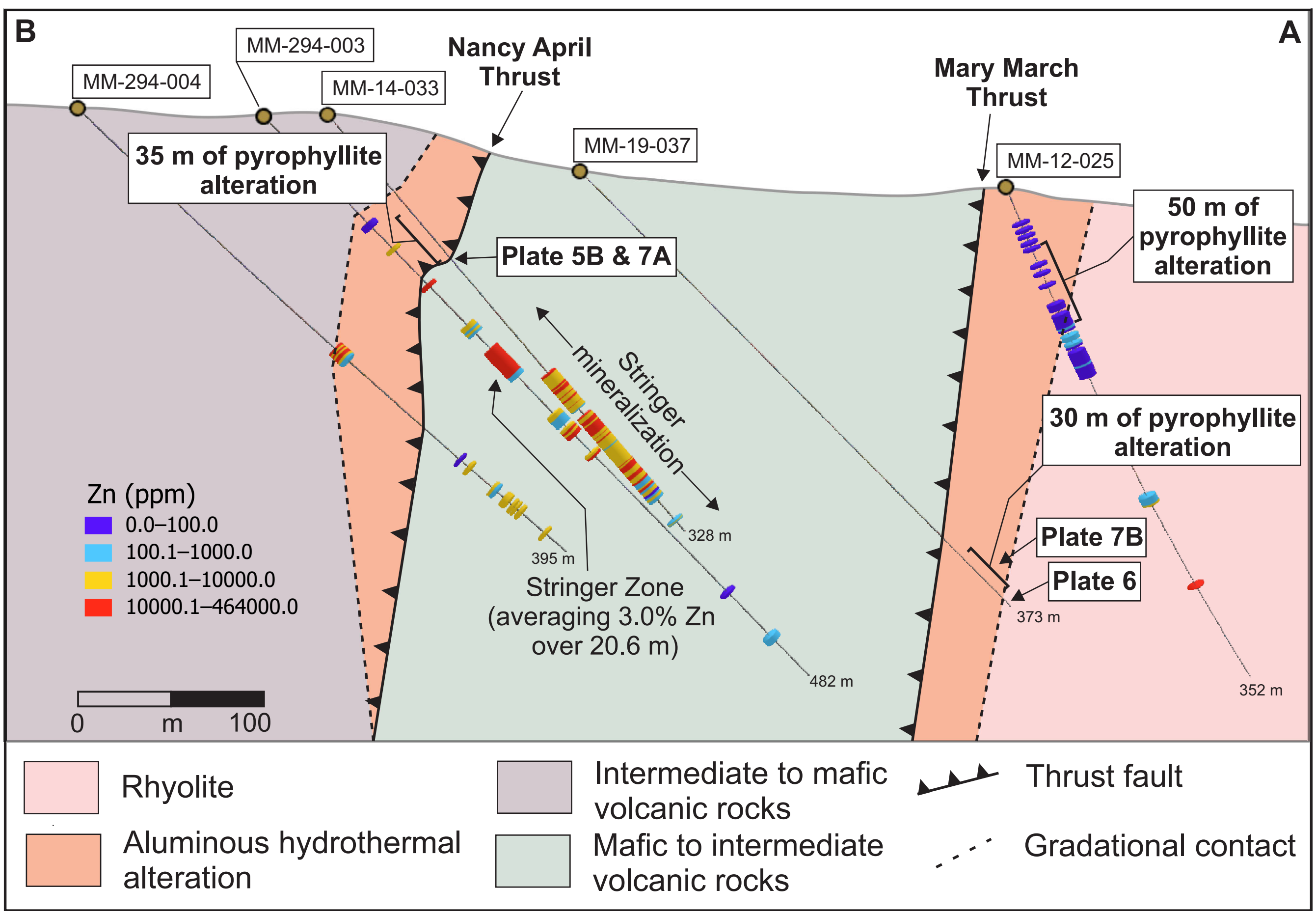

Figure 13. *Schematic cross-section of the Mary March prospect, outlining the distribution of zinc values from industry assay data relative to significant fault structures and identified zones of advanced argillic alteration based on spectral data (note drill-holes MM-294-004 & 003 were not examined with SWIR). For the location of the section* see *Figure 12 (bottom right, cross-section A-B). Assay data compiled from Jagodits and Thurlow (2000), Green and Wolfson (2013) and Oosterman (2015).*

(Plate 6), is primarily restricted to the footwall zone of the Mary March thrust. The development of pyrophyllite alteration displays a spatial association with the contact zone between this unit and overlying intermediate to felsic lapilli tuff and tuff breccia (*see* below).

Massive sulphide mineralization generally occurs in structurally complex zones proximal to thrust faults in the area, along with stringer- and locally replacement-style sulphide mineralization developed within both mafic and felsic volcanic rocks in the structural footwall of both the Nancy April and Mary March thrust faults. To date, the thickest intersection of massive sulphide comes from the immediate footwall zone of the Mary March thrust fault, which returned 10.1% Zn, 1.7% Pb, 0.6% Cu, 122.1 g/t Ag and 4.2 g/t Au over 9.6 m (Jagodits and Thurlow, 2000). Here, high-grade massive sulphide is interbedded with mineralized lithic material and more massive pyrite, but is highly disrupted due to faulting and the intrusion of post-mineralization mafic and felsic dykes, which also intrude along the fault structures. Another intersection along strike to the northeast contained significant gold enrichment, assaying 12.2 g/t Au and 660 g/t Ag in association with 16.8% Zn, 3.5% Pb and 0.2% Cu over 0.9 m (Thurlow, 2001); the mineralized interval was also associated with elevated As (699 ppm), Cd (414 ppm) and Sb (97 ppm). In contrast, the massive sulphide mineralization identified in the hanging wall of the Nancy April thrust fault largely consists of massive pyrite, locally associated with anomalous Au (up to 330 ppb), Ag (up to 14 g/t), Se (up to 92 ppm) and Te (up to 30 ppm; Oosterman, 2015). The pyrite-dominated lens, traced for approximately 250-m along strike, varies in thickness from 1.6 to 6.5 m, and is spatially associated with strong paragonite–paragonitic illite–montmorillonite argillic alteration of the footwall rocks (*see* below). The structural panel between the two thrust faults is host to well-developed stringer- and replacement-style mineralization, hosted within mafic to intermediate volcanic rocks, locally returning intersections of up to 1.0% Zn, 0.2% Pb and 2.9 g/t Ag over 93.7 m (DDH MM-14-033; Figure 13; Oosterman, 2015).

Plate 6. *Well-developed flow banding and perlitic fracturing within phengite-altered rhyolite of the footwall zone to the Mary March thrust fault; DDH MM-19-037, 367 m depth, Mary March prospect.*

Aluminous alteration in the form of pyrophyllite and alunite has been identified throughout the area (*see* Sparkes 2022, and references therein), locally displaying a spatial association with VMS-related mineralization. Geochemical samples of the alteration from earlier exploration programs returned values of up to 41% Al_2O_3 (Thurlow, 1999), indicating the aluminous nature of the alteration in this area. Although early interpretations assumed the alteration represented a later overprinting-event superimposed on the VMS mineralization, recent SWIR investigations demonstrate the alteration is more widespread and is synchronous with VMS mineralization. Pyrophyllite-dominated alteration assemblages have been identified in the hanging wall to the Nancy April thrust fault (Plate 7A), where it has been traced over 1.3 km of strike length, and both pyrophyllite (Plate 7B) and alunite occur within the footwall of the Mary March thrust fault, where it has been traced for over 0.9 km, along strike. This alteration is typically barren with respect to base and precious metals, however the transition up-section and along strike into paragonite–paragonitic illite–montmorillonite-dominated argillic alteration has returned assays of up to 2.5% Cu, 0.1% Zn, 8.6 g/t Ag and 0.7 g/t Au over 2.3 m (Plate 8; Oosterman, 2015). This mineralized zone is also associated with elevated As (up to 1.1%), Bi (up to 48 ppm), Hg (6 ppm), Mo (up to 13 ppm), Sb (up to 95 ppm), Se (up to 216 ppm) and Te (up to 146 ppm).

SWIR INVESTIGATIONS OF FOOTWALL ATLTERATION ZONE

Mary March Prospect

The SWIR investigations of the Mary March prospect highlight several dominant alteration assemblages related to the development of argillic and advanced argillic alteration in the area. The footwall rocks to the Mary March thrust fault are characterized by phengitic white mica alteration, distal from the main zone of advanced argillic alteration. Here, the phengite-altered intermediate to felsic lapilli tuff and tuff breccia quickly transition through muscovitic illite into paragonite–paragonitic illite–pyrophyllite-advanced argillic alteration over a span of approximately 20 m (Figure 14; Plate 7B). The development of this advanced argillic alteration is centred on the contact between the underlying flow-banded rhyolite and overlying intermediate hyaloclastite and lapilli tuff. Within the central core of the advanced argillic alteration, the protolith hosting the alteration is uncertain due to the intensity of the alteration. This zone highlights the shift of the Al-OH scalar from ~2220 to ~2193 nm, at the core of the advanced argillic zone (Figure 14). Below the advanced argillic alteration, the white mica alteration transitions back into muscovitic illite and then to phengite (Plate 6), and the Al-OH values return to longer spectral wavelengths (~2220 nm). Unfortunately, in the location of the cross-section outlined in Figure 13, no VMS mineralization develops in association with the advanced argillic or the marginal argillic alteration within the footwall of the Mary March thrust fault. However, based on industry

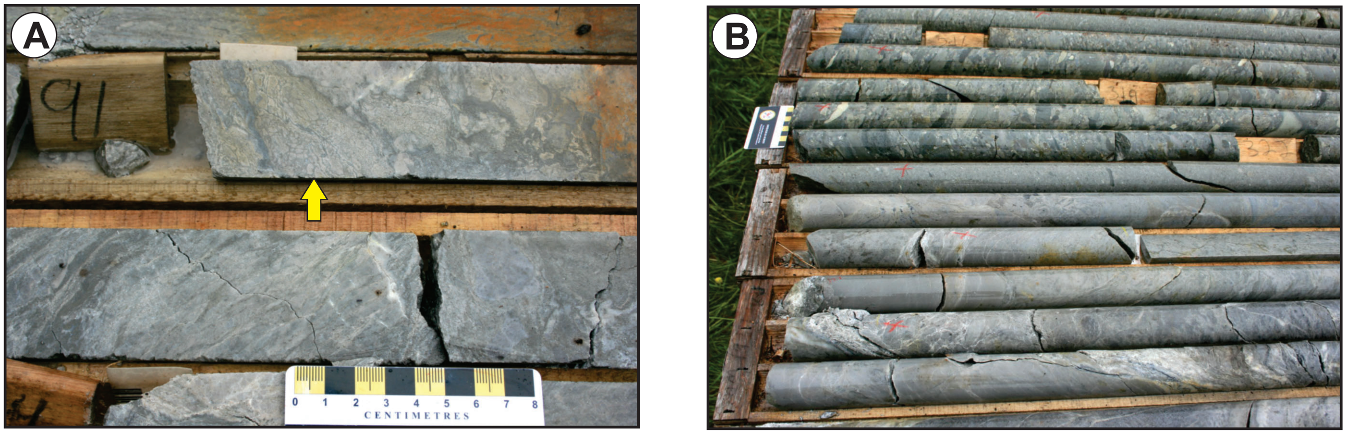

Plate 7. *A) Pyrophyllite-altered intermediate to felsic tuff breccia hosting relic perlitic-fractured felsic clast (yellow arrow) displaying a similar texture to that observed in the footwall rhyolite (Plate 6); hanging wall of the Nancy April thrust fault (Figure 13). DDH MM-14-033, 91 m; B) Photograph of the transition from phengitic white mica-altered lapilli tuff (top) through muscovitic illite and then into pyrophyllite–paragonite–paragonitic illite moving downhole toward the footwall rhyolite shown in Plate 6 (Figure 13); DDH MM-19-037, 320 m depth, Mary March prospect.*

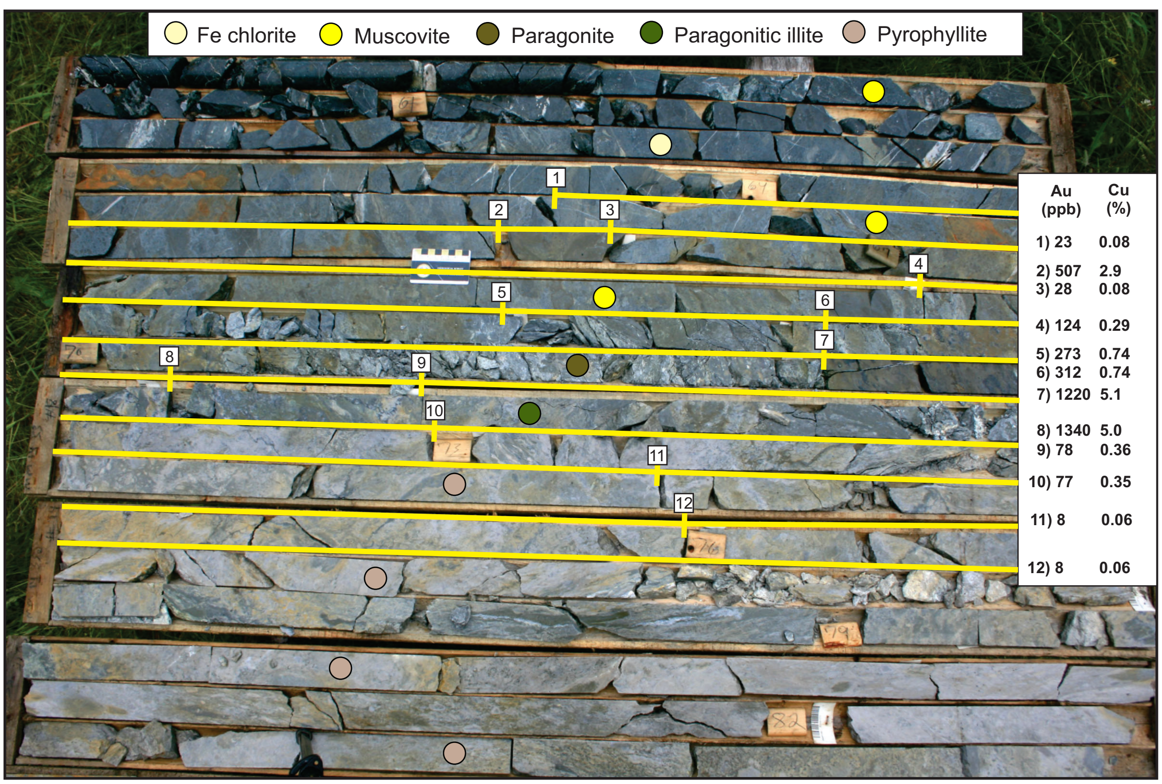

Plate 8. *Transitional zone showing the gradational change from chlorite-altered intermediate hyaloclastite into pyrophyllite-altered felsic to intermediate tuff breccia. Also shown are the industry gold and copper assay values from Oosterman (2015) and spectra location sites with corresponding mineralogy. DDH MM-14-033, 59 to 83 m depth, Mary March prospect.*

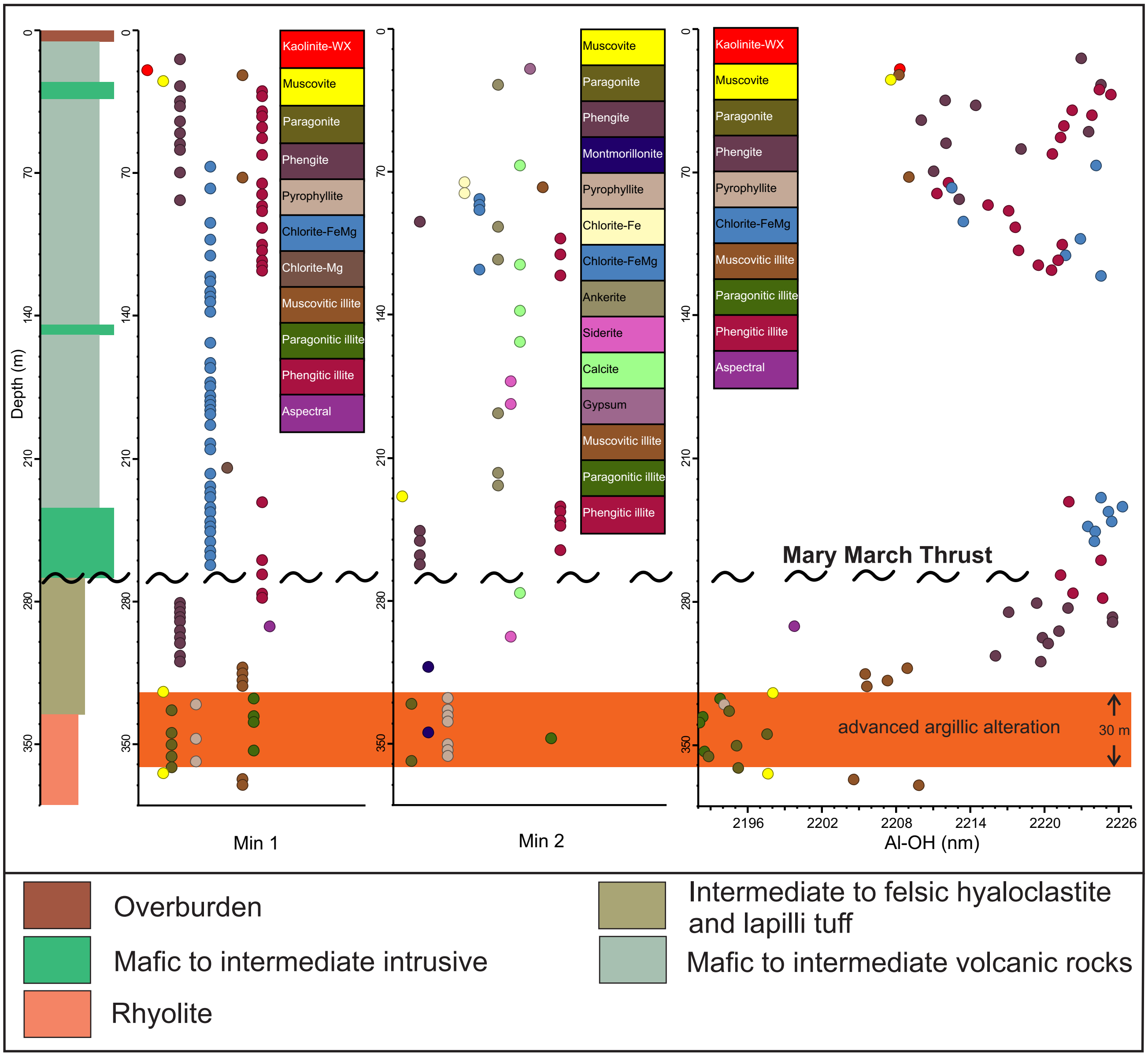

Figure 14. *Strip log for DDH MM-19-037 outlining the zonation of the white mica alteration below the Mary March thrust, marginal to pyrophyllite-dominated advanced argillic alteration; Mary March prospect. Min 1 and Min 2 represent the two most abundant minerals based on the spectral data as determined from the TSG results. The variation in the calculated Al-OH scalar is shown.*

reports and sections (*e.g.*, Jagodits and Thurlow, 2000), mineralization is developed in a similar stratigraphic setting within the footwall zone approximately 500 m along strike to the northeast. A drillhole that undercut the main mineralized intersection in the area to the northeast was investigated using SWIR (DDH MM-19-036; not shown), but it predominantly contained phengite-altered felsic volcanic rocks within the footwall zone of the Mary March thrust fault, suggesting the mineralized horizon is structurally truncated at depth.

Situated structurally above the footwall intermediate to felsic volcanic rocks, is a mafic- to intermediate-dominated volcanic sequence (structural hanging wall; stratigraphic footwall; see below) which is characterized by Fe-Mg chlorite and lesser phengite and phengitic illite alteration. These rocks are separated from the underlying sequence by the Mary March thrust fault (Figure 14). The structural hanging-wall rocks are host to stringer- and local-replacement-style VMS mineralization, associated with Fe-Mg chlorite alteration (Figure 13). These rocks represent the country rock into which the footwall rhyolite unit is emplaced based on regional outcrop relationships, and given the associated style of mineralization observed within the sequence, it is interpreted to represent the stratigraphic footwall. Upper portions of this structural panel contain moderate to strong phengite to phengitic illite white mica alteration, proximal to the Nancy April thrust fault. This phengitic alteration also displays a spatial association with the intrusion of intermediate dykes within the mafic volcanic rocks. These intermediate dykes are of similar composition to the intermediate hyaloclastite volcanic rocks within the same sequence and are inferred to be co-magmatic.

The advanced argillic alteration occurring within the structural hanging wall of the Nancy April thrust fault is inferred to represent a structurally repeated zone similar to that developed beneath the Mary March thrust fault. Within the structural hanging wall of the Nancy April thrust fault, intermediate to felsic tuff breccia, locally containing felsic fragments displaying well-developed perlitic fracturing (Plate 7A), is host to pyrophyllite-dominated advanced argillic alteration, up to 35 m thick (Figure 13). Here, copper–gold-dominated VMS-related mineralization occurs at the transition from the advanced argillic into the marginal argillic alteration (Plate 8). This mineralization is also associated with anomalous silver, arsenic, bismuth, mercury, molybdenum, antimony, selenium, and tellurium. Locally developed massive pyrite, presumed to be of an exhalative origin, is located 150 m along strike to the southwest in a similar stratigraphic setting to that shown in Plate 8. Here, the massive pyrite mineralization is underlain by paragonite–paragonitic illite–montmorillonite argillic alteration hosted in intermediate to felsic lapilli tuff, before the alteration is truncated along the Nancy April thrust fault (Plate 9; Figure 15). Immediately below the thrust fault are mafic to intermediate volcanic rocks hosting Fe-Mg chlorite and phengitic alteration along with local stringer- and replacement-style VMS mineralization. These rocks represent the same sequence occurring within the hanging wall of the Mary March thrust fault (Figure 13).

The SWIR investigations of the footwall rocks to the Mary March thrust indicate an overall transition from pyrophyllite-dominated advanced argillic alteration in the northeast to pyrophyllite–kaolinite–alunite-dominated assem-

Plate 9. *Massive pyrite (top), inferred to be exhalative in origin, located above 10 m of intense paragonite–paragonitic illite–montmorillonite footwall alteration as shown in Figure 15; the alteration is locally host to clasts of massive pyrite (red arrow). This alteration represents the same stratigraphic interval shown in Plate 8, but located 150 along strike to the southwest. The zone does not contain any significant enrichment in base metals, but the massive pyrite displays anomalous enrichment in Au (up to 326 ppb), Ag (up to 14.2 g/t), Se (up to 92 ppm) and Te (up to 30 ppm). Note the location of the Nancy April thrust fault is shown by the yellow arrow. DDH MM-14-035, 63 to 87 m depth, Mary March prospect.*

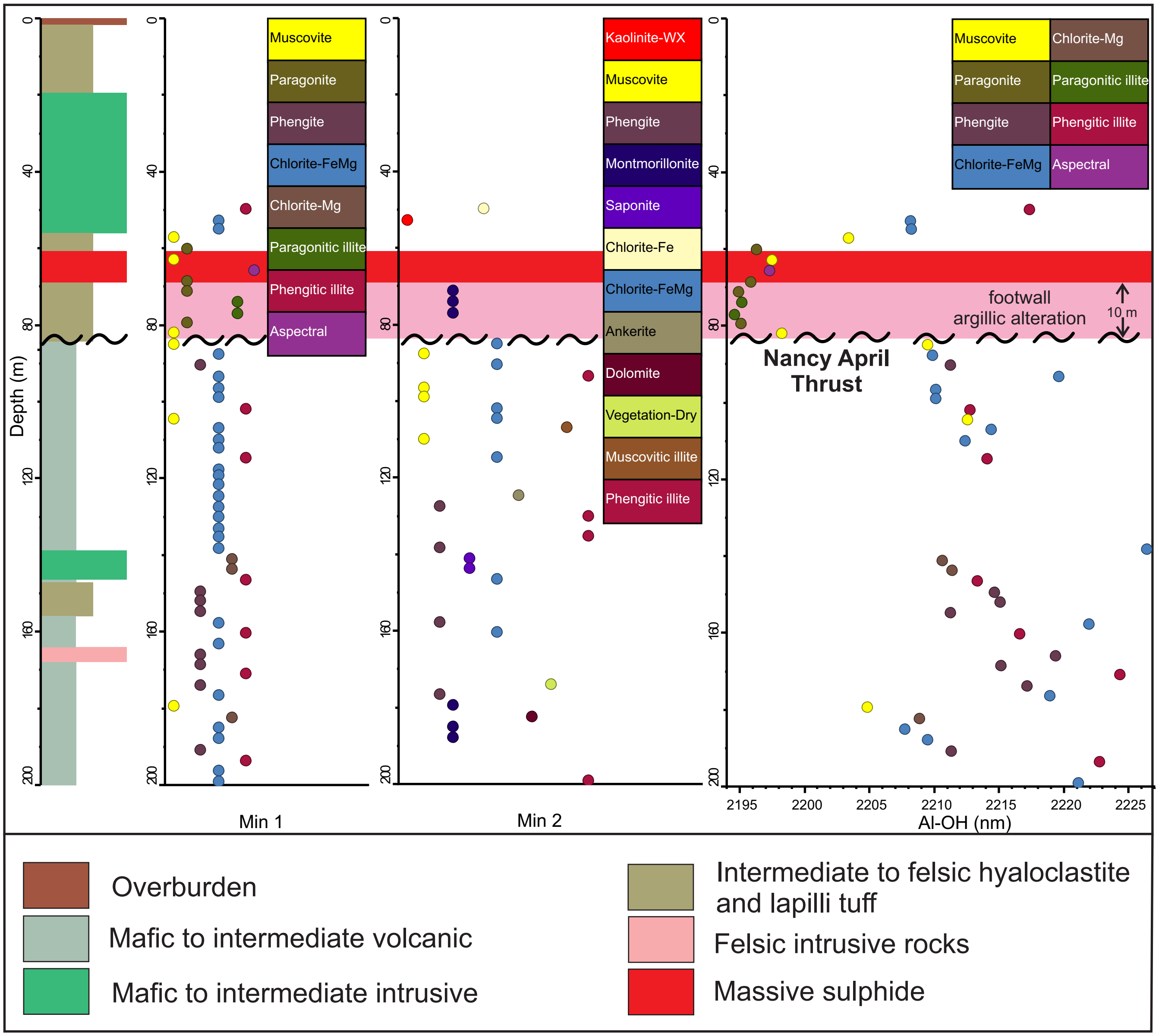

Figure 15. *Strip log for DDH MM-14-035, located 150 m along strike to the southwest of hole MM-14-033 shown in Figure 13. This hole intersected massive pyrite in association with footwall argillic alteration immediately above the Nancy April thrust fault; Mary March prospect. Min 1 and Min 2 represent the two most abundant minerals based on the spectral data as determined from the TSG results. The variation in the calculated Al-OH scalar is shown.*

blages in the southwest. However, no such variation has been identified within the hanging-wall zone of the Nancy April thrust fault, where the advanced argillic alteration is only noted to contain pyrophyllite. In the southwestern part of the Mary March prospect, the alteration within the footwall of the Mary March thrust fault displays a zonation from muscovite–paragonite–pyrophyllite, transitioning up section into kaolinite–alunite and then into relatively unaltered phengitic intermediate volcanic rocks (DDH BJ-074; Sparkes, 2022). Here, the footwall-advanced argillic alteration is up to 65 m thick (core length); this alteration is located some 800 m to the southwest of the section shown in Figure 13. The alteration within the structural hanging wall of the Nancy April thrust fault in the southwestern portion of the prospect is predominated by paragonite but still contains rare pyrophyllite (*e.g.*, DDH BJ-065; Sparkes, 2022), indicating a transition to lower temperature, less acidic hydrothermal conditions to the southwest within this structural panel.

DISCUSSION

Within the TVB and BRAB, the local development of extensive zones of advanced argillic alteration, in association with felsic volcanism, highlights the presence of significant hydrothermal systems. Here, VMS mineralization displays a spatial association with the development of these hydrothermal systems, albeit somewhat removed from the acidic, high-temperature portion of the overall system. Within the region, the main zones of advanced argillic alteration are generally devoid of significant VMS mineralization, which is instead associated with marginal argillic-dominated assemblages generally situated some distance along strike of the advanced argillic alteration. In addition, the characterization of spectral data from the footwall-alteration zone of massive sulphide mineralization as being dominated by shorter wavelength white mica minerals (*e.g.*, paragonite, paragonitic illite, muscovite and muscovitic illite) and montmorillonite, is a common feature in some deposits associated with this style of mineralization (*e.g.*, Daniels Pond, Bobbys Pond, and the Nancy April zone of the Mary March prospect). A similar mineral zonation is also noted within the immediate footwall rocks of the high-grade Lucky Strike deposit of the Buchans camp (Sparkes, 2022 and references therein), which also displays evidence of potential magmatic–hydrothermal fluid input (van Hees, 2011).

The distinct mineral zonation patterns associated with the footwall environment also can be used to indicate the overall younging direction of the hydrothermal systems in overturned terrains (*e.g.*, Daniels Pond deposit). Likewise, distinct mineral assemblages also can be utilized to identify the hanging-wall environment, such as the local abundance of carbonate that displays a spatial association with the mineralized horizon or the immediate hanging wall (*e.g.*, Daniels Pond and Bobbys Pond deposits). The spatial association of carbonate with such zones of acidic alteration could be indicative of fluid mixing between the acidic hydrothermal fluids and seawater (*see* Williams and Davidson, 2004).

The systematic variation of the Al-OH wavelength feature provides some insight to the changing hydrothermal conditions proximal to zones of advanced argillic alteration and VMS mineralization. The shift to shorter wavelength white mica minerals (*e.g.*, paragonite and muscovite) illustrate the increasingly acidic hydrothermal conditions associated with mineralization in hybrid bimodal-felsic VMS systems within the region. In addition, sharp shifts in the Al-OH values measured from drillcore generally indicate the presence of a significant fault structure, which results in the juxtaposing of contrasting hydrothermal conditions (*i.e.*, temperature, acidity).

The enrichment of the typical epithermal suite of elements (*e.g.*, As, Bi, Hg, Sb, Se, Sn and Te) associated with the hybrid bimodal-felsic style of VMS mineralization within both the TVB and BRAB is supportive of a magmatic contribution to the hydrothermal fluids associated with the formation of these systems. This is further supported by the precious-metal enrichment, locally associated, with the development of VMS mineralization (*e.g.*, Daniels Pond, Mary March prospect).

In the TVB, the identification of hybrid bimodal-felsic-hosted VMS mineralization occurring intermittently (?) over approximately 8 km illustrates the potential of the belt to host such styles of mineralization. In addition to the known deposits and prospects that display such alteration characteristics, further work is warranted on a number of other occurrences in the general vicinity, including the Jacks Pond deposit and associated Cathy's Pond prospect occurring approximately 8 km to the southwest of the Daniels Pond deposit (Figure 2). The Jacks Pond deposit is associated with the largest known alteration system in the TVB; yet no detailed and systematic study has been conducted on the alteration mineralogy. Additionally, the North Pond prospect, in close proximity to the Bobby's Pond sulphur prospect (~2 km to the northeast) contains massive pyrite in association with intense silicification, alunite and minor native sulphur alteration, and represents another area with potential for further research.

Within the BRAB, the recent recognition of this style of mineralization, combined with SWIR investigations of drillcore and outcrops within the region provide a new way of evaluating hydrothermal alteration. Such investigations highlight areas with prospective mineralogy, such as the Tower prospect (Figure 12; Sparkes, 2022), which is associated with a recently identified zone of pyrophyllite alteration exposed over 60 m in width at surface, but has received minimal exploration both in the immediate area and along strike. Likewise, continued exploration along strike to the southwest of the Mary March prospect, along the defined airborne magnetic low associated with the hydrothermal alteration, represents a prospective environment for VMS mineralization, which is further supported by untested coincident barium and gold surficial geochemical anomalies.

CONCLUSION

The SWIR investigations of aluminous alteration associated with hybrid bimodal-felsic VMS mineralization within the TVB and BRAB, demonstrate several common characteristics associated with the development of these hydrothermal systems. Advanced argillic alteration assemblages (pyrophyllite ± dickite ± kaolinite ± alunite) highlight hotter, more acidic zones of these hydrothermal systems, which generally are not well mineralized. Instead, massive sulphide mineralization is commonly developed marginal to such zones, under less acidic and potentially lower temperature hydrothermal conditions. Such relationships, combined with detailed alteration mapping of SWIR may help direct future exploration in these regions toward prospective mineralizing environments.

The investigation of the footwall environment to VMS mineralization, associated with hybrid bimodal-felsic-type systems within the TVB and BRAB has identified several common mineral assemblages within these environments. Within the footwall region, and locally, the immediate hanging wall, the Al-OH wavelength feature displays a distinct zonation from longer wavelength white mica minerals, distal to mineralization and associated alteration, to shorter wavelength white mica minerals in more proximal settings. These features, combined with the local enrichment of the epithermal suite of elements, provide vectors that are not commonly applied to exploration for the more typical styles of VMS-related mineralization.

ACKNOWLEDGMENTS

Emily Scott is thanked for assisting in the field and diligent efforts in the collection of spectral data, and Gerry Hickey is thanked for providing logistical support. William Oldford is gratefully acknowledged for his assistance in the Buchans core library. Canstar Resources is thanked for providing access to drillcore.

REFERENCES

Agnerian, H.
2007: Technical report on the Bobby's Pond Cu-Zn deposit, Newfoundland and Labrador, Canada. Prepared for Mountain Lake Resources Inc. NI 43-101 Report Update, 111 pages.

AusSpec International Ltd.
2008: Spectral analysis guides for mineral exploration (GMEX): Practical applications handbook. 3rd edition.

Barbour, D.M., Desnoyers, D.W., Dunphy, B.A., Graves, R.M., Kieley, J.W., King, B.M., McKenzie, C.B., Poole, J.C. and Thurlow, J.G.
1991: Assessment report on geological, geochemical, geophysical, trenching and diamond drilling exploration for 1990 submission for the Anglo-Newfoundland Development Company Limited Charter, crown lease lots A-B, E-F and P-R, fee simple grants volume 1 folios 43, 61-62 and 110, volume 2 folios 23 and 25, special volume 2 folio 307 and Reid Lots 227-228, 231-233 and 247 in the Buchans, Great Burnt Lake, Valentine Lake, Victoria Lake, Tulks River and Lloyds River areas, central Newfoundland, 6 reports. Newfoundland and Labrador Geological Survey, Assessment File 12A/0609, 2134 pages.

Barbour, D.M., Desnoyers, D.W., Graves, R.M., Kieley, J.W., King, B.M., McKenzie, C.B., Poole, J.C., Thurlow, J.G., Balch, S. and MacNeil, J.
1990: Assessment report on geological, geochemical, geophysical, trenching and diamond drilling exploration for the Victoria Lake project for 1989 submission for the Anglo-Newfoundland Development Company Limited charter, Reid lots 227-228, 231-233 and 247, fee simple grants volume 1, folios 43, 61 and 110 and volume 2 folios 23 and 29 and for crown lease lots A, B, E, J and N to R in the Buchans, Red Indian Lake, Valentine Lake, Jacks Pond and Daniels Pond areas, central Newfoundland, 5 reports. Newfoundland and Labrador Geological Survey, Assessment File NFLD/1970, 1260 pages.

Bell, R., Watson, D., Gillham, S. and Ryan, O.
1989: Fourth year assessment report on geological, geochemical, geophysical and diamond drilling exploration for the Victoria project for licence 3351 on claims 14609-14616, 15264-15268 and 15534-15542 and on claim blocks 1212, 1601, 4028-4031, 4107-4111 and 4382-4386 in the Bobbys Pond and Victoria River areas, central Newfoundland, 4 reports. Newfoundland and Labrador Geological Survey, Assessment File 12A/10/0526, 954 pages.

Brueckner, S.M., Piercey, S.J., Pilote, J.-L., Layne, G.D. and Sylvester, P.J.
2016: Mineralogy and mineral chemistry of the metamorphosed and precious metal-bearing Ming deposit, Canada. Ore Geology Reviews, Volume72, pages 914-939.

Brueckner, S.M., Piercey, S.J., Sylvester, P.J., Maloney, S. and Pilgrim, L.
2014: Evidence for syngenetic precious metal enrichment in an Appalachian volcanogenic massive sulfide system: The 1806 Zone, Ming Mine, Newfoundland, Canada. Economic Geology, Volume 109, pages 1611-1642.

Dadson, P., Woods, D.V. and Fedikow, M.
2004: Fifth year and fifth year supplementary assessment report on prospecting and geochemical, geophysical and diamond drilling exploration for licences 6575M, 9054M, 9726M and 9731M on claims in the

Jacks Pond, Daniels Pond and Bobbys Pond areas, central Newfoundland. Newfoundland and Labrador Geological Survey, Assessment File 12A/1188, 290 pages.

Galley, W.D., Hannington, M.D. and Jonasson, I.R.
2007: Volcanogenic massive sulphide deposits. *In* Mineral Deposits of Canada: A Synthesis of Major Deposit-types, District Metallogeny, the Evolution of Geological Provinces, and Exploration Methods. *Edited by* W.D. Goodfellow. Mineral Deposits Division, Geological Association of Canada, Special Publication 5, pages 141-161.

Gifkins, C., Herrmann, W. and Large, R.
2005: Altered volcanic rocks: a guide to description and interpretation. Centre for Ore Deposits Research, University of Tasmania, Australia, 275 pages.

Gill, S.B., Piercey, S.J. and Layton-Matthews, D.
2016: Mineralogy and metal zoning of the Cambrian Zn-Pb-Cu-Ag-Au Lemarchant volcanogenic massive sulfide (VMS) deposit, Newfoundland. The Canadian Mineralogist, Volume 54, pages 1307-1344.

Green, B.J. and Wolfson, I.
2013: First year supplementary assessment report on diamond drilling exploration for licence 20398M on claims in the Buchans Junction area, central Newfoundland. Newfoundland and Labrador Geological Survey, Assessment File 12A/15/1651, 116 pages.

Halley, S.W., Dilles, J.H. and Tosdal, R.M.
2015: Footprints: Hydrothermal alteration and geochemical dispersion around porphyry copper deposits. SEG Newsletter, Issue Number 100, pages 11-17.

Hannington M.D., Poulsen K.H., Thompson J.F.H. and Sillitoe R.H.
1999: Volcanogenic gold in the massive sulfide environment. *In* Volcanic-Associated Massive Sulfide Deposits: Processes and Examples in Modern and Ancient Settings. *Edited by* C.T. Barrie and M.D. Hannington. Society of Economic Geologists, Littleton, CO, USA, pages 325-356.

Hedenquist, J.W. and Arribas, A.
2022: Exploration implications of multiple formation environments of advanced argillic alteration. Economic Geology, Volume 117, pages 609-643.

Herrmann, W., Blake, M., Doyle, M., Huston, D., Kamprad, J., Merry, N. and Pontual, S.
2001: Short wavelength infrared (SWIR) spectral analysis of hydrothermal alteration zones associated with base metal sulfide deposits at Rosebery and Western Tharsis, Tasmania, and Highway-Reward, Queensland. Economic Geology, Volume 96, pages 939-955.

Hinchey, J.
2011: The Tulks Volcanic Belt, Victoria Lake Supergroup, central Newfoundland – geology, tectonic setting and volcanogenic massive sulphide mineralization. Government of Newfoundland and Labrador, Department of Natural Resources, Geological Survey, Report 2011-02, 185 pages.

Huston, D.L. and Kamprad, J.
2001: Zonation of alteration facies at Western Tharsis: Implications for the genesis of Cu-Au deposits, Mount Lyell Field, Western Tasmania. Economic Geology, Volume 96, pages 1123-1132.

Jagodits, F.L. and Thurlow, J.G.
2000: Assessment report on geological, geochemical, geophysical and diamond drilling exploration for 1999 submission for the Anglo-Newfoundland Development Company Limited Charter, fee simple grant Volume 2 Folio 29 and Reid Lot 247, and for first and ninth year assessment for licence 4117 on claim block 8058 and licences 6967M-6970M on claims in the Buchans Junction area, central Newfoundland, 2 reports. Newfoundland and Labrador Geological Survey, Assessment File 12A/1026, 342 pages.

McKenzie, C., Desnoyers, D., Barbour, D. and Graves, M.
1993: Contrasting volcanic-hosted massive sulphide styles in the Tulks Belt, central Newfoundland. Exploration and Mining Geology, Volume 2, Number 1, pages 73-84.

Noranda Ltd.
1998: Precious and base metal properties available for option in central Newfoundland. Summary Report, ca. 500 pages.

Oosterman, D.
2015: Third year assessment report on geophysical and diamond drilling exploration for licence 20398M on claims in the Buchans Junction area, central Newfoundland. Newfoundland and Labrador Geological Survey, Assessment File 12A/15/1693, 231 pages.

Pilote, J.-L., Piercey, S.J., Brueckner, S.M. and Grant, D.
2016: Resolving the relative timing of Au enrichment in volcanogenic massive sulfide deposits using scanning electron microscopy-mineral liberation analyzer:

Empirical evidence from the Ming deposit, Newfoundland, Canada. Economic Geology, Volume 111, pages 1495-1508.

Pontual, S., Merry, N. and Gamson, P.
1997: G-Mex volume 1: Spectral interpretation field manual; Arrowtown, New Zealand, Ausspec International Pty. Ltd., 86 pages.

Regular, M.
2006: Assessment report on diamond drilling exploration for 2005 submission for Mining Lease 187 [4881] in the Bobbys Pond area, central Newfoundland. Newfoundland and Labrador Geological Survey, Assessment File 12A/10/1271, 132 pages.

Sawitzky, E. and Dadson, P.
2003: Fourth year assessment report on geological, geochemical, geophysical and diamond drilling exploration for licences 9040M-9041M and 9054M on claims in the Sutherlands Pond, Daniels Pond and Roebucks Brook areas, central Newfoundland. Newfoundland and Labrador Geological Survey, Assessment File 12A/1041, 538 pages.

Sillitoe, R.L., Hannington, M.D. and Thompson, J.F.H.
1996: High-sulfidation deposits in the volcanogenic massive sulphide environment. Economic Geology, Volume 91, pages 204-212.

Sparkes, G.W.
2022: Short wavelength infrared spectrometry studies of sericitic alteration zones, southern Buchans-Roberts Arm Belt, Newfoundland. *In* Current Research. Government of Newfoundland and Labrador, Department of Industry, Energy and Technology, Geological Survey, Report 22-1, 34 pages.

Squires, G.C., Brace, T.D. and Hussey, A.M.
2001: Newfoundland's polymetallic Duck Pond deposit: Earliest Iapetan VMS mineralization, formed within a sub-seafloor, carbonate-rich alteration system. *In* Geology and Mineral Deposits of the Northern Dunnage Zone, Newfoundland Appalachians. *Edited by* D.T.W. Evans and A. Kerr. GAC/MAC Field Trip Guide A2 (Part 1), pages 167-187.

Stewart, R. and Beischer, G.
1993: The Bobbys Pond base metal sulphide deposit, Victoria property, central Newfoundland. *In* Ore Horizons. *Edited by* A. Hogan and H.S. Swinden. Government of Newfoundland and Labrador, Department of Mines and Energy, Geological Survey Branch, Volume 2, pages 89-100.

Thurlow, J.G.
1999: Assessment report on geological, geochemical and diamond drilling exploration for 1998 submission for the Anglo-Newfoundland Development Company Limited Charter, fee simple grant Volume 2 Folio 29 and Reid Lot 247, and for third and eighth year assessment for licence 4117 on claim block 8058 and licence 4763M on claims in the Buchans Junction area, central Newfoundland. Newfoundland and Labrador Geological Survey, Assessment File 12A/1025, 38 pages.

2001: Assessment report on diamond drilling exploration for 2000 submission for the Anglo-Newfoundland Development Company Limited Charter in the Buchans Junction area, central Newfoundland. Newfoundland and Labrador Geological Survey, Assessment File 12A/15/1166, 121 pages.

van Hees, G.W.
2011: Chemostratigraphy and alteration geochemistry of the Lundberg and Engine House volcanogenic massive sulfide mineralization, Buchans, central Newfoundland. Unpublished M.Sc. thesis, University of Ottawa, Ottawa, ON, 178 pages.

Williams, N.C. and Davidson, G.J.
2004: Possible submarine advanced argillic alteration at the basin lake prospect, western Tasmania, Australia. Economic Geology, Volume 99, pages 987-1002.

Yang, K., Huntington, J.F., Gemmell, J.B. and Scott, K.M.
2011: Variations in composition and abundance of white mica in the hydrothermal alteration system at Hellyer, Tasmania, as revealed by infrared reflectance spectroscopy. Journal of Geochemical Exploration, Volume 108, pages 143-156.

Zagorevski, A. and Rogers, N.
2008: Stratigraphy and structural geology of the Ordovician volcano-sedimentary rocks in the Mary March Brook area. *In* Current Research. Government of Newfoundland and Labrador, Department of Natural Resources, Geological Survey, Report 08-1, pages 101-113.

2009: Geochemical characteristics of the Ordovician volcano-sedimentary rocks in the Mary March Brook area. *In* Current Research. Government of Newfoundland and Labrador, Department of Natural Resources, Geological Survey, Report 09-1, pages 271-288.

Zagorevski, A., McNicoll, V.J., Rogers, N. and van Hees, G.H.
2016: Middle Ordovician disorganized arc rifting in the peri-Laurentian Newfoundland Appalachians: implica-

tions for evolution of intra-oceanic arc systems. Journal of the Geological Society, Volume 173, pages 76-93.

Zagorevski, A., McNicoll, V., van Staal, C.R., Kerr, A. and Joyce, N.
2015: From large zones to small terranes to detailed reconstruction of an Early to Middle Ordovician arc-backarc system preserved along the Iapetus suture zone: A legacy of Hank Williams. Geoscience Canada, Volume 42, pages 125-150.

Zagorevski, A., Rogers, N., van Staal, C., McClenaghan, S. and Haslam, R.
2007: Tectonostratigraphic relationships in the Buchans area: a composite of Ordovician and Silurian terranes? *In* Current Research. Government of Newfoundland and Labrador, Department of Natural Resources, Geological Survey, Report 07-1, pages 103-116.

Zagorevski, A., Rogers, N., van Staal, C.R., McNicoll, V., Lissenberg, C.J. and Valverde-Vaquero, P.
2006: Lower to Middle Ordovician evolution of peri-Laurentian arc and backarc complexes in Iapetus; constraints from the Annieopsquotch accretionary tract, central Newfoundland. Geological Society of America Bulletin, Volume 118, pages 324-342.